Measurement Report: Interpretation of Wide Range Particulate Matter Size Distributions in Delhi

Ülkü Alver Şahin[1], Roy M Harrison[2,a], Mohammed S. Alam[2,b]
David C.S. Beddows[2,3], Dimitrios Bousiotis[2], Zongbo Shi[2]
Leigh R. Crilley[4], William Bloss[2], James Brean[2], Isha Khanna[5,c]
and Rulan Verma[6,c]

[1] Istanbul University-Cerrahpaşa, Engineering Faculty, Environmental
Engineering Department, Istanbul, Türkiye

[2] School of Geography, Earth and Environmental Sciences
University of Birmingham, Birmingham, B15 2TT, UK

[3] National Centre for Atmospheric Science
University of York, Heslington, York, YO10 5DQ, UK

[4] Department of Chemistry, York University
Toronto, Ontario, M3J 1P3, Canada

[5] Puget Sound Clean Air Agency, Seattle, Washington, USA 98101

[6] Institute of research on catalysis and the environment of Lyon - IRCELYON
Université De Lyon, 69626 Villeurbanne cedex, France

Corresponding author: E-mail: r.m.harrison@bham.ac.uk (Roy M. Harrison)

[a] Also at: Department of Environmental Sciences / Centre of Excellence in Environmental
Studies, King Abdulaziz University, PO Box 80203, Jeddah, 21589, Saudi Arabia

[b] Now at: School of Biosciences, University of Nottingham, Sutton Bonington
Campus, Leicestershire, LE12 5RD

[c] Previously at: IIT Delhi, Hauz Khas, New Delhi, India 110016

ABSTRACT

Delhi is one of the world's most polluted cities, with very high concentrations of airborne particulate matter. However, little is known on the factors controlling the characteristics of wide range particle number size distributions. Here, new measurements are reported from three field campaigns conducted in winter, pre-monsoon and post-monsoon seasons on the Indian Insitute of Technology campus in the south of the city. Particle number size distributions were measured simultaneously using a Scanning Mobility Particle Sizer and a Grimm optical particle monitor, covering 15 nm to >10 µm diameter. The merged, wide-range size distributions were categorised into five size ranges: nucleation (15-20 nm), Aitken (20-100 nm), accumulation (100 nm-1 µm), large fine (1-2.5 µm) and coarse (2.5-10 µm) particles. The ultrafine fraction (15-100 nm) accounts for about 52 % of all particles by number (PN_{10}-total particle number from 15 nm to 10 µm), but just 1 % by PM_{10} volume (PV_{10}- total particle volume from 15 nm to 10 µm). The measured size distributions are markedly coarser than most from other parts of the world, but are consistent with earlier cascade impactor data from Delhi. Our results suggest substantial aerosol processing by coagulation, condensation and water uptake in the heavily polluted atmosphere, which takes place mostly at nighttime and in the morning hours. Total number concentrations are highest in winter, but the mode of the distribution is largest in the post-monsoon (autumn) season. The accumulation mode particles dominate the particle volume in autumn and winter, while the coarse mode dominates in summer. Polar plots show a huge variation between both size fractions in the same season and between seasons for the same size fraction. The diurnal pattern of particle numbers is strongly reflective of a road traffic influence upon concentrations, especially in autumn and winter, although other sources such as cooking and domestic heating may influence the evening peak. There is a clear influence of diesel traffic at nighttime when it is permitted to enter the city, and also indications in the size distribution data of a mode <15 nm, probably attributable to CNG/LPG vehicles. New particle formation appears to be infrequent, and in this dataset is limited to one day

65   in the summer campaign. Our results reveal that the very high emissions of airborne particles in

66   Delhi, particularly from traffic, determine the variation of particle number size distributions.

67

1.   INTRODUCTION

Air pollution in Delhi has been studied for many years, and the authorities have implemented several interventions designed to limit the concentrations. The sulphur content of diesel and petrol fuels was reduced to 50 ppm during 1996-2010, more than 1300 industries were shut down due to hazardous emissions, commercial vehicles older than 15 years were gradually taken out of the traffic fleet, and public transport vehicles and auto-ricksaws were converted to compressed natural gas (CNG) fuel (Narain and Krupnick, 2007). An odd–even vehicle number plate restriction has been applied during working days (Chowdhury et al., 2017). Although these measures have reduced gaseous pollutants (SO_2 and CO) and primary particulate matter, in recent years, several studies have reported that the $PM_{2.5}$ concentrations have been constant or slowly increasing in India, especially in the winter and autumn seasons (Babu et al., 2013; Balakrishnan et al., 2019; Dandona et al. 2017, Kumar et al., 2017), except in 2020. In 2020, the $PM_{2.5}$ level decreased by approximately 40 %, due to Covid-19 measures (Rodríguez-Urrego and Rodríguez-Urrego 2020; Mahato et al., 2020). Although the overall emission sources in India are dominated by traffic, industry, construction, and local biomass burning, haze pollution events in Delhi are frequently related to the large-scale open burning of post-harvest crop residues/wood during the crop burning season in nearby rural regions (Cusworth et al. 2018; Bikkina et al. 2019; Kanawade et al., 2020). Furthermore, the sources of particles are mostly local (Hama et al., 2020), meteorological factors play an important role in influencing concentrations of air pollution (Tiwari et al., 2014; Yadav et al., 2016; Guo et al., 2017; Dumka et al. 2019; Kumar et al. 2020).

Annual average $PM_{2.5}$ levels range between 81 and 190 $\mu g/m^3$ in Delhi and are clearly higher than the WHO guideline value (5 $\mu g/m^3$) and Indian national limit value (40 $\mu g/m^3$) (Hama et al., 2020). To the best of our knowledge, most studies in India have focussed on the source apportionment from chemical profiles of particles (Pant and Harrison, 2012; Jain et al. 2020; Bhandari et al., 2020; Rai et al., 2020). Mostly they have reported that biomass burning contributes greatly to $PM_{2.5}$ mass while

traffic contributes heavily to PM_{10} mass in Delhi. Residential energy use contributes 50 % of the $PM_{2.5}$ mass concentration and the construction sectors are also considered an important source of particle mass (Guttikunda et al., 2014; Butt et al., 2016; Conibear et al., 2018). Furthermore, it is particularly important to understand the absolute contribution and sources of different sizes of particles within $PM_{2.5}$. A recently published paper by Das et al. (2021) highlighted that <250 nm particles contribute a significant proportion of the total $PM_{2.5}$ mass and are a potentially important link with human health.

The Particle Number Size Distribution (PNSD) can provide air pollution source apportionment with high time resolution compared to use of chemical species, and influences the aerosol transport and transformation profiles in the urban atmosphere and toxicological effects on humans (Wu and Boor, 2021). Many PNSD studies have been conducted in urban, traffic and background sites over the past decades and three review studies have been published (Vu et al., 2015; Azimi et al., 2014; Wu and Boor, 2021). There are some studies evaluating the number or mass particle size distribution (PSD) in Delhi (Mönkkönen et al., 2005; Chelani et al., 2010; Gupta et al., 2011; Pant et al., 2016; Gani et al., 2020). Harrison (2020) compared PNSDs from Delhi, Beijing and London and reported that the particles from Delhi are far greater in number with a much larger modal diameter, close to 100 nm. In a recent paper, Gani et al. (2020) has investigated the PNSD up to 0.5 µm sizes from 2017 to 2018 and reported that rapid coagulation is an important process in Delhi.

The wide range PNSD is important to describe all sources of inhalable particles (<10 µm). It is not easy to separately identify particles arising from resuspension, sea salt and construction, or from brake wear and combustion or vehicle exhaust, using only the <0.5 µm particle size range. Harrison et al. 2011 reported that using wide range particle sizes in source apportionment was extremely successful in identifying the separate contributions of on-road emission including brake wear and resuspension. Although there are a few studies of wide range particle characterization in Beijing (Jing et al., 2014)

120 and source apportionment in Venice, Italy (Masiol et al., 2016), there has been no previous wide

121 range PNSD study in Delhi. In this study, we aimed to interpret particulate matter size distributions

122 over a wide range (15 nm to 10 µm) in the winter, post-monsoon and pre-monsoon seasons in Delhi.

123 Future studies will look at two-step receptor modelling of wide range particulate matter size

124 distributions and chemical composition in Delhi.

125

126 **2.   METHODS**

127 **2.1   Study Area**

128 The measurements were part of the NERC/MoES Air Pollution and Human Health in an Indian mega-

129 city (APHH-Delhi, www.urbanair-india.org) study, a joint UK-India project addressing air pollution

130 in Delhi. The sampling location was ~15 m above ground level on the 5th floor of the Civil

131 Engineering Department at the Indian Institute of Technology Delhi (IIT Delhi) campus, located in

132 New Delhi, representative of an urban background environment (28.545 N, 77.193 E) (Figure S1).

133 The measurement station is at a 120 m distance from a major arterial road. As part of APHH-Delhi,

134 there were three field campaigns: (i) Jan-Feb 2018 (winter), (ii) May-June 2018 (summer; pre-

135 monsoon) and (iii) Oct-Nov 2018 (autumn; post-monsoon). In all field campaigns, a suite of gas and

136 particulate phase instrumentation was deployed within a temperature controlled laboratory.

137

138 These sampling periods were representative of conditions for PM and gases during these seasons in

139 Delhi. We found the average $PM_{2.5}$ concentration to be approximately 180 µg/m^3, 220 µg/m^3 and 120

140 µg/m^3 for winter, autumn (excluding Diwali) and summer, respectively measured by a TEOM-FDMS

141 (TEOM-Filter Dynamic Measurement System). Hama et al. (2020) studied the long term (from 2014

142 to 2017) trends of air pollution in Delhi at 6 stations (residential, commercial, and industrial sites)

143 and reported that the mean $PM_{2.5}$ concentrations ranged between 147 – 248 µg/m^3, 147 – 248 µg/m^3

144 and 76 – 135 µg/m^3 for winter, autumn and summer, respectively, and a good correlation between

145 sites within Delhi. This gives reassurance that the $PM_{2.5}$ concentrations measured at our site are within

146 the typical range of those observed in Delhi.

147

148 **2.2   Measurements**

149 Aerosol particle sizes in the atmosphere span a very wide range from a few nanometers at the lower

150 end to some tens of micrometers at the upper end. Because of this very wide range of sizes, particle

151 properties vary considerably across the size spectrum with the behaviour of the smaller particles being

152 determined by their high mobility and hence diffusivity, whilst at the coarse end of the size

153 distribution inertial properties are especially important. Due to this divergence in behaviour, no

154 instrument is capable of measurement of the whole range of particle sizes.

155 To measure the particle size range used in this study, two particle instruments were used to collect

156 number size distributions (NSD). For the range 15-640nm, a TSI- Scanning Mobility Particle Sizer

157 (SMPS) 3936 was used, consisting of a TSI 3080 Electrostatic Classifier, TSI 3081 DMA and TSI

158 3775 CPC. To extend this range into the coarse mode a Portable Laser Aerosol Spectrometer and

159 Dust Monitor (GRIMM 1.108) were used alongside the SMPS.

160

161 **2.3   Merging Process**

162 Merging procedures have usually been reported for merging SMPS and APS (Aerosol Particle Sizer)

163 data, but here Grimm optical spectrometer (OP) data is merged with SMPS data. For a complete

164 particle size distribution, simultaneously collected, paired hourly averaged particle number size

165 distributions collected from the SMPS and Grimm were merged. The merging procedure is based on

166 the principle of converting the diameters of the Grimm-derived data to a diameter matching the

167 SMPS-derived data, in the region where the size distribution measurements overlap. The Grimm

168 measures the optical diameter d_b^t whereas the SMPS measures the mobility diameter d_a^t of the

169 particles. Comprehensive descriptions of the procedure and mathematics are given by DeCarlo et al.

170 (2004) and Schmid et al. (2007). The Grimm NSD are translated onto the extended electical mobility

diameter axis of the SMPS using equation (R1) (Beddows et al. 2010; Liu et al., 2016; Ondracek et al., 2009).

$$d_b^t = \frac{d_a^t}{X} \sqrt{\frac{C(d_a^t)}{C(d_b^t)}} \qquad (R1)$$

The Cunningham slip correction factor is given by C and the unknown variables such as the shape factor of the particles are accounted for by a free parameter X (given by equation R2) which is adjusted until the tails of the SMPS and Grimm NSD overlap each other giving a continuous NSD across the particle size bins measured by the two instruments.

$$X = \sqrt{\frac{\rho_e^t}{\rho_o}} \qquad (R2)$$

The estimated transition-regime effective density ρ_e^t (normalised by the unit density, ρ_o) typically ranges from 0.77 to 2.56 g/cm^3 when aerodynamic diameter is used in merging. Detailed information upon the effective particle density based on the geographical regions is seen in the Wu and Boor (2021) study.

The merging algorithm (originally programmed in CRAN R) was implemented using Excel spreadsheets and the solver tool minimised the separation between the tails of the overlapping SMPS and Grimm. Due to the imperfect nature of the data, each of the merges was allocated a factor indicating quality based on whether: (i) there is a successful fit; (ii) the scatter of the data across the overlapping tails; (iii) the fraction of points on the tail falling onto the fitted curve; and (iv) how smooth the overlap is (Table S1). The size bins overlap (300-700 nm) between Grimm and SMPS. This process was repeated for the winter, summer and autumn data sets and any results failing the test

were either repeated or the data removed from the analysis. In all, only 8 samples from 1117 failed to give an acceptable fit in the merge procedure.

2.4 Data and Quality Management

Data from SMPS and Grimm were measured with 1-min resolutionand converted to hourly averages. The seasons were categorized as winter, autumn and summer. The measurements were taken in winter from 12 January 16:00 to 11 February 04:00, in autumn from 24 October 16:00 to 11 November 10:00, in summer 16 May 19:00 to 05 June 15:00 in 2018. There were 709, 403 and 477 total pairs (hours) in the data sets in winter, autumn and summer, respectively. But 172, 43 and 257 pairs in winter, autumn and summer, respectively were excluded because of the non-availability of data at that time. Data coverage is 76 % for winter, 95 % for autumn and 46 % for summer. Figure S2 in the Supplementary shows hourly mean values of total particle counts for three seasons. In order to evaluate day and night time PNC (particle number concentration) differences, the day and night were defined as 07:00-19:00 and 19:00 – 07:00, respectively. All times reported are local times recorded in Indian Standard Time (IST; GMT+05:30).

R version 3.1.2 was used to analyse the data (R Core Team, 2015). Firstly, all data were checked for clean-up of the robustness of the data sets, to detect anomalous records and take out the extreme values. Data greater than the 99.5th percentile were deleted. Diwali time in 2018 (7th of November 2018 from 16:00 to 23:00) was taken out the date set in order to exclude its extreme effect on PNSD values. Particle number concentrations during Diwali time are given in the Supplementary, Figure S3. There were some single gaps in the data matrixes. These missing data were replaced by linearly interpolated values from the nearest bins to those samples.

In the literature, PNCs measured below 1 µm are frequently split into three ranges: nucleation, Aitken and accumulation (Gani et al., 2020). Nucleation size ranges have variously been described as below

221   30 nm (Masiol et al. 2016) or below 25 nm (Gani et al., 2020) or below 20 nm (Wu and Boor, 2021).

222   Some studies have evaluated wide range PNSDs split into 4 ranges (nucleation, Aitken, accumulation

223   and coarse) (Masiol et al. 2016; Harrison et al., 2011). In this study, the modes have been aggregated

224   into five size groups: nucleation (15-20 nm), Aitken (20 -100 nm), accumulation (100 nm – 1 µm),

225   large fine (1 µm – 2.5 µm) and coarse (2.5 µm – 10 µm) based on merged. Ultrafine particles (UFP)

226   are considered to be total PN counts of Nucleation and Aitken modes (<100 nm).

227

228   The particle mass was calculated for the SMPS+OP merged data, assuming a density of 1.6 g cm^{-3}

229   (Gani et al., 2020). Estimation of particle density as a function of size is extremely difficult, and there

230   are few data for particle density from Delhi. Since Gani et al (2020) used the density of PM at the

231   same location as in our study, we used the same density value to convert PN to PM mass. Figure S4

232   shows the comparison of PM$_{2.5}$ measured by SMPS+OP and TEOM-FDMS in Delhi for the three

233   seasons. Figure S5 shows the comparison of PM$_{2.5}$ with relative humidity measured by SMPS+OP

234   and TEOM in Delhi for the three seasons. A good correlation of the estimated particle mass with

235   independent measurements with a co-located TEOM-FDMS was observed, except in summer.

236

237   The cumulative frequency of observations as a function of particle size was calculated for each hour

238   of the day. Standard central measures from the cumulative frequency plots were represented by the

239   geometric mean diameter (GMD) for each size distribution. They were used to examine particle

240   growth processes. Firstly, the growth of GMD was estimated visually from the diurnal GMD data

241   plot (Fig. 8). The minimum growth time used for estimation of the growth rate (GR) was selected as

242   three hours, and if the growth lasted for long enough, the GR was estimated. The observed growth of

243   the GMD of the particle was quantified by fitting the GMD of particles during the growth process

244   event over a period of time 't' (eq.1). Detailed information on the method can be found in Sarangi et

245   al. (2015; 2018).

246

247 Growth rates (nm/hour)-GR =dGMD/dt (1)
248

249 **3. RESULTS**

250 **3.1 Particle Number and Size**

251 Table S2 gives the descriptive statistics of particle number counts ($\#/cm^3$) calculated using every 1-

252 hour measurements for the nucleation, Aitken, accumulation, large fine and coarse modes between

253 15 nm and 10 µm in all seasons. Time series of total particle number counts are presented in Figure

254 S2. The average total PN levels were 36.73×10^3 cm^{-3} in winter, 29.35×10^3 cm^{-3} in autumn and

255 18.91×10^3 cm^{-3} in summer. Generally, the wintertime PN levels were higher than the other seasons.

256 The wintertime PN levels of nucleation, Aitken and accumulation modes were ∼1.5, 1.8 and 2.2 times

257 higher than in summer, respectively. Similar ratios were obtained by Guttikunda and Gurjar (2012)

258 in Delhi for particulate matter concentrations. This is attributed to the unfavorable dispersion

259 conditions, including low wind speed and low mixing height during the winter season. The autumn

260 PN levels of nucleation, Aitken and accumulation modes were ∼1.5, 1.3 and 1.9 times higher than in

261 summer, respectively. The wintertime and autumn average PN levels are similar except for the Aitken

262 mode for which winter is 1.4 times higher than in autumn. However, for the large fine and coarse

263 modes the PN level was not markedly different between winter, autumn, and summer. Gani et al.

264 (2020) reported that the average PN levels were 52.50×10^3 cm^{-3} in winter, 43.40×10^3 cm^{-3} in

265 summer, and 38.00×10^3 cm^{-3} in autumn in Delhi measured in 2017. The differences in the magnitude

266 of number counts between the two studies are potentially explained by the difference in the sampling

267 period and changes in emissions.

268

269 Figure 1 shows a comparison of average particle number and volume and the contribution to total

270 PN. The average PV (particle volume) levels indicate that PV of the Aitken mode is highest in winter,

271 while the accumulation mode is highest in autumn and the coarse mode is highest in summer. The

272 contribution of UFP to numbers is highest in summer (57 %) but their contribution to volume is the

273 lowest in autumn and summer (<1 %). The contribution to both number and volume of the

accumulation mode is highest in autumn with 51 % and 75 %, respectively. UFP contributions to total PV are below 1 % in Delhi. Furthermore, it can be seen clearly that the coarse fraction of particles dominates in summer, while the accumulation mode dominates in autumn and winter.

Wu and Boor (2021) analysed the PNSD observations made between 1998 and 2017 in 114 cities in 43 countries around the globe. They reported that there are significant variations in the magnitude of urban aerosol PNSD among different geographical regions. The main finding of their study is that the PNSD in Europe, North America, Australia, and New Zealand are dominated by nucleation- and Aitken-mode particles while in Central, South, Southeast and East Asia they are dominated by the substantial contribution from the accumulation mode, which is consistent with our finding. Pant et al. (2016) report mass size distributions for particulate matter sampled by cascade impactor in Delhi in winter. The dominant modes appear at around 3-4 µm and 0.6 µm, with a lesser peak at 0.2 µm aerodynamic diameter. These are respectively in the coarse (former mode) and accumulation (latter two modes) ranges as classified in the current study. The largest component of mass was in the accumulation mode, and the distribution fits well with the pattern of data seen in Figure 1. Major components of the coarse fraction were Al, Si, Ca and Fe (Pant et al., 2016), suggestive of soil and street dust as major contributors. The elements most notably in the accumulation fraction were Cu, Zn, Pb and Sb, indicative of non-exhaust traffic emissions and metallurgical sources, and S, which showed a major peak due to sulphate, peaking at 0.9 µm (Pant et al., 2016).

3.2   Diurnal Change

Figure 2 shows the diurnal variation of particle number concentrations and of $PM_{2.5}$, BC, NO and NO_2 for each season (excluding the day of Diwali), and the normalized time variations of all particle fractions are given in Figure S6. Figure S7 represents the diurnal variation of meteorological parameters. In general, there are large differences of PN levels between cold seasons (winter and autumn) and warm season (summer) for nucleation size particles. Coarse mode particle numbers in

the summer are higher than in winter and autumn, except in the evening time. For autumn and winter, particle counts are similar from 7 am to 7 pm (daytime). However, from 7 pm to 7 am particle counts in winter are higher than in autumn. The lowest levels for all modes were present during the afternoon in all seasons (2-4 pm), followed by highest levels during the night in winter (after 8 pm). The winter and autumn diurnal profiles had two peaks for below 1 µm particle size in the morning and evening corresponding to the traffic rush hours. But in the summer the same peaks for nucleation, Aitken and accumulation modes are seen although of smaller magnitude, and one hour earlier comparing to the winter and autumn. Pant et al. (2016) reported the diurnal variation of traffic at one of the major arterial roads in Delhi and Dhyani et al. (2019) reported on traffic-related emission. Figure S9 shows the diurnal variation in traffic at a major road intersection in Delhi. Cars, two/three wheelers, bus and LCV (light commercial vehicle) fleet numbers increase in the morning, persist throughout daytime and start to decrease at 22:00. Due to the prohibition of access for heavy-duty diesel vehicles to central Delhi from 6:00 am until 11:00 pm in the night, during the daytime including the traffic rush hours the HCV (heavy commercial vehicles) number is at its lowest level (Figure S9 or Dhyani et al. 2019). While road traffic clearly influences the diurnal pattern in PN, other sources including cooking and domestic combustion are likely to contribute. Small midday PN peaks were observed during the summer in the nucleation, Aitken and coarse modes. Another study conducted in Delhi reported the same midday peaks in the warm season and the highest levels in the cold season (Gani et al. 2020), which may be related to bus and LCV emissions at midday.

Figure 3 shows the differences in diurnal variations of total PN levels between the weekday and weekend. These are based upon a small dataset, and hence the rather small differences within a season may not be meaningful. In winter the PN levels on Saturday and Sunday are higher than on the weekdays during the night (from 8 pm to 10 am the next day). However, after the morning rush hour peaks, during the daytime the PN levels are the same for all days. The diurnal variation of PN in the autumn shows no significant differences among the days with the same main peaks in the morning

for all days, although highest on Saturday. There is a flattened peak (from 8 to 10 am) in the morning rush hour for the weekday while there are pointed peaks at approximately 9 am on Saturday and Sunday in winter and autumn. Measurements made during the summer period are very limited. Due to there being only 4 full days and 9 half days of measurements, it is very hard to draw any conclusions. Even so, there are indications of a weekday traffic effect upon the PN levels in summer. There is only one day of measurements on a Sunday (3rd June 2018) and it shows the midday peaks. Overall, despite seasonal differences, there appears to be a strong influence of light duty road vehicles upon the diurnal profiles, reflecting traffic volumes, with an impact of heavy duty vehicles upon nighttime concentrations of all particle fractions.

NPF events present variable seasonality for different areas, though in most cases they appear to be more frequent during spring or summer (Salvador et al., 2021). Gani et al. 2020 studied long term PNSD in Delhi and have stated that they did not see any NPF during the winter or autumn seasons in Delhi. In this study, the identification of NPF events was conducted manually using the criteria set by Dal Maso et al. (2005) and used by Bousiotis et al (2019; 2021). The data were analysed visually on a day-to-day basis: each 24-hour period, from midnight to midnight. According to these criteria, a NPF event is considered when: a distinctly new mode of particles appears in the nucleation mode size range, prevails for some hours, and shows signs of growth. These are the initial criteria used in identifying the events. Following that, as the dataset starts from a rather large size (15 nm), to be more confident about the events and not to confuse them with pollution events, high time resolution data for NO_x as well as the fluctuations of the condensation sink were also used to identify pollution events affecting particle concentrations which were not considered. Hence, while we checked the particle size distributions for the NPF events, we also looked at the levels of pollutants to ensure that what was attributed to a NPF event was not particles from pollution / direct emissions. By considering the pollution levels and condensation sink we can reduce the possibility of including particle formation events that are not associated with secondary formation. After analysing all data,

measurements from only one day during the measurement campaign were compliant with the criteria set as a class Ia NPF event. Figure 4 presents the contour plots of average diurnal variation for all seasons and for the NPF event on 3rd June. NPF may be suppressed due to very high pre-existing aerosol concentrations (Kanawade et al., 2020; Gani et al. 2020) during severe air pollution episodes in Delhi. This suppression effect has also been observed in European cities (Bousiotis et al., 2019; 2021).

A new study by Sebastian et al. (2021) analysed PNSD and the frequency of NPF at six different locations in India. The Delhi observation site is in an urban area and located at CSIR-National Physical Laboratory (NPL), approximately 8 km from the IIT location described as urban background in our study. They found that the NPF frequently occurs in the spring season, but is least common in autumn and winter due to air pollution episodes suppressing the NPF. They also stated that the highest concentration and frequency of occurrence of NPF events in was Delhi as compared to other sites. As in other studies (such as Bousiotis et al., 2021), this study also emphasized that the increased concentrations of precursor gases are important for the occurrence of NPF in urban areas.

3.3   Day and Night Time Differences in PN and PV

Table S3 presents the summary statistics of the particle number and mass levels derived from merged particle number data and BC, NO_x and $PM_{2.5}$ at night and day for each season, excluding Diwali. Figure 5 shows the particle number comparison of all modes at night and day seasonally. In both night and day, the nucleation counts are approximately the same in autumn and summer (N/D=1.1 and 1.0), and a little higher at night in winter (N/D=1.3). But in the night, Aitken and accumulation counts are higher than in the day by factors of 1.4 and 1.5 times in summer, 1.2 and 1.5 times in autumn, respectively and approximately 2 in winter. While the coarse mode PN counts are approximately the same for all seasons and day / night, the large fine PN level in the nighttime are significantly higher (1.7) than in the daytime in summer. It seems that in the nighttime high PM concentrations are due to the increasing Aitken and accumulation modes occurring from coagulation

380 of nucleation mode particles, condensation of low volatility species or hygroscopic growth. In

381 addition, biomass burning and older diesel vehicles can contribute significantly to particles in these

382 fractions (Kumar et al., 2013; Chen et al., 2017; Gani et al., 2020). Meteorological factors can also

383 profoundly affect the PN levels in daytime and nighttime. The differences of wind speed between day

384 and night in summer are lower than in winter and autumn (Figure S7). Higher wind speed, and lower

385 humidity, may favour the resuspension of coarse dust as a dominant mechanism in the summer.

386 Seasonal changes in mixing depths are surprisingly small (Figure S7) and hence unlikely to have a

387 major influence. However, the major increases and decreases in the diurnal plots of pollutants (Figure

388 2) are consistent with the diurnal plots of MLH (Figure S7). Autumn and winter also have longer

389 periods with low mixing heights, also seen in Figure S7. TPN showed a negative exponential

390 dependence upon MLH, which became more scattered at lower values of MLH, probably reflecting

391 the larger relative errors in MLH estimates at smaller values.

392

393 Figure S8 represents the relation between the ventilation coefficients (VC = MLH $\times$ wind speed) and

394 TPN as a function of hour and month. Gani et al. (2019) reported that the VC is 4–6 times smaller for

395 the wintertime compared to the summer in Delhi. In this study, the VC is 1.8 and 1.6 times higher in

396 summer (mean 2732 m^2/s) compared to the winter (mean 1491 m^2/s) and autumn (mean 1702 m^2/s),

397 respectively. The daytime hourly TPN levels are lower as related to the higher VC and the lower VC

398 in colder months gives higher TPN. Although there are not enough daily data (especially for summer)

399 to give more detail, we can see the same trend as comparing to the weekly data from Gani et al (2019)

400 study.

401

402 Overall, for the daytime for all seasons, hourly averaged UFP concentrations are usually less than

403 the nighttime, however the UFP contribution to the PN_1 (55 % in day, 50 % in night for winter; 52

404 % in day, 45 % in night for autumn; 58 % in day, 56 % in night for summer) and PN_{10} (38 % in day,

405 38 % in night for winter; 40 % in day, 33 % in night for autumn; 36 % in day, 33 % in night for

summer) are mostly slightly higher in the daytime. Similarly, Gani et al. (2020) have reported the highest contribution (of UFP to PNC) in the daytime compared with the nighttime in Delhi. Due to the difference of PN size range (they measured down to 12nm), they found the UFP contribution to PNC higher than in the present study.

3.4 Size Distributions

Figure 6 shows the average PNSD in three seasons in Delhi. Volume and Area distributions are shown in the Supplementary Materials in Figure S10. The highest number concentrations are seen in winter, followed by autumn, and then summer. Although the number concentrations of particles below 200 nm are far greater in winter those between 200 and 600nm are greater in autumn, within the accumulation mode. The winter and summer PNSD show modes at approximately 100 nm but the autumn PNSD shows the mode at approximately 200 nm. This could be due to changing sources of particles in Delhi between seasons (Jain et al. 2020), in addition to (differing) aerosol dynamical processes. The Delhi atmosphere is more polluted comparing with most other cities based on particle number and mass (Harrison, 2020). This will cause a tendency for particles to grow more rapidly by coagulation and condensation (Harrison et al., 2018), but this might be expected to occur in all seasons.

As described above, in Delhi the nighttime particle concentrations are markedly higher than the daytime concentrations. The PNSD changes for each hour of the day across all three seasons were analysed (Figure S11) and categorized. Figure 7 presents the PNSD differences between daytime and nighttime and shows the variation in PNSDs within the day in all seasons. The main difference between day and night in winter is only the number concentration, with little change in the mode size between day and night, while the PNSDs in summer and autumn show bimodal distributions with modes at approximately 30 and 140 nm in summer, and 35 and 200 nm in autumn. When we focus on PNSD during the daytime, it can be clearly seen that the modes are manifest at different times: In

432   winter, while the PNSD shows the same mode at approximately 100 nm from 8 am to 2 pm, the mode

433   in the afternoon (from 2 pm to 6 pm) drops slightly in size (70 nm). In the morning and afternoon

434   there are two small peaks at 60 nm and 40 nm for the Aitken fraction and 170 and 130 nm for the

435   accumulation fraction in autumn. During the day in summer, there are two peaks at approximately 30

436   nm from 10 am to 6 pm. This may be associated with summer nucleation events and NPF on 3rd June

437   2018 (Figure 4). Furthermore it may be related to the growth of particles from 10 am to 2 pm in

438   autumn and summer. The full reasons for these changing PNSDs are not clear, and it would be unwise

439   to attempt a detailed interpretationof a very small dataset.

440

441   Figure 8 shows the average geometric mean diameter (GMD) change with hour of the day. Two

442   overall periods of GMD increase are observed. One of them is in nighttime in all seasons with GMD

443   growing at between 4.6 nm/hour in summer and 6.2 nm/hour in winter. The particle growth in autumn

444   is predominantly (when compared to the winter and summer) both late in the night (from 0 am to 5

445   am) and in the morning (from 8 am to 12 pm). Considering the PNSD trend in autumn (Figure 7), the

446   GMD rises at 9 nm/hour from morning to noon. Similar results were obtained in the USA (Kuang et

447   al., 2012), Canada (Jeong et al., 2010; Iida et al. 2008), Italy (Hamed et al., 2007) and Japan (Han et

448   al. 2013). However the calculated GMD growth rate is smaller than that calculated by Sarangi et al.,

449   (2015; 2018) in Delhi, by Kalafut-Pettibone et al. (2011) in Mexico City and by Zhang et al. (2011)

450   in Beijing. The changing GMD with time in Delhi could be the result of changing sources, and/or of

451   dynamics. Nocturnal growth may be the result of reducing temperatures and increasing RH causing

452   vapour condensation (Sarangi et al., 2018). Morning growth may be due to oxidation processes

453   leading to production of less volatile vapours which then condense onto the particles (Sarangi et al.

454   2018).

455

456   Figure 9 gives the average particle number, volume, area and mass size distribution for all seasons.

457   While the number size distributions have one mode, two peaks are observed in volume distributions,

458   centered at 0.5 µm and 6 µm. These relate to two different main sources, which might be secondary

459   aerosol (such as sulphate at high RH) in the fine mode and road dust resuspension, soil or construction

460   dust for the coarse mode (Pant et al. 2016). In winter and autumn fine mode particle volumes are

461   higher than the coarse mode. However, in summer the coarse mode particle volumes are higher than

462   the fine particle level. In a recent paper, Thamban et al. (2021) show that modes in the mass size

463   distributions of hydrocarbon organic aerosol (HOA), Semi-volatile oxygenated organic aerosol

464   (SVOOA), biomass burning organic aerosol (BBOA) and low-volatile oxygenated organic aerosol

465   (LVOOA) measured by aerosol mass spectrometry are typically in the range 300-600nm vacuum

466   aerodynamic diameter, very consistent with the peaks seen in the mass distributions in Figure 9.

467

468   Hama et al. (2020) obtained the spatiotemporal characteristics of daily-averaged air pollutants and

469   concluded that the particulate matter mass (PM_{10} and $PM_{2.5}$) is dominated by local sources across

470   Delhi. The main local air pollutant sources in Delhi include traffic, construction, resuspension of dust,

471   diesel generators, power plants, industries and biomass burning (Kumar et al., 2013; Nagpure et al.,

472   2015; Hama et al., 2020).

473

474   All average PNSD graphs show an increasing trend in PNC at particle sizes below 19 nm particle

475   diameter. SMPS measurements in this study were conducted only above 15 nm. So, the peak particle

476   size within this size range cannot be seen. However, the clear increase in particle number below 19

477   nm indicates that another source may be important in Delhi. This small mode and bimodal PNSD

478   during the day (Figure 7) may be associated with the road transport vehicle types in Delhi. Despite

479   the diesel restriction during the rush hours and conversion of the public transport vehicles to CNG,

480   several studies have reported that $PM_{2.5}$ concentrations have been remaining steady or are slowly

481   increasing in India, especially in the winter and autumn seasons (Babu et al., 2013; Balakrishnan et

482   al., 2019; Dandona et al. 2017; Kumar et al., 2017).

483

The fuels used in Delhi's traffic fleet are petrol, diesel, CNG and LPG. Legislation limits the sulphur content of the fuel to 50 ppm in diesel as per Bharat Stage IV. The diesel vehicles are not required to be fitted with particle traps. The technology of the gasoline vehicle fleet varies as vehicle engine capacity changes. Cars, two/three wheelers, bus and LCV fleet volumes are high during the day. Due to the time restrictions on trucks/heavy good vehicles entering the city, during the daytime the HCV number is at its lowest level (Figure S9).

Previous published studies indicate that emissions of particles from CNG vehicles (Euro 4, 5, 6) with diameter greater than 23 nm are as low as a diesel particle filter equipped vehicle, and an order of magnitude lower than gasoline vehicles (Kontses et al. 2020; Giechaskiel, et al. 2019; Magara-Gomez et al. 2014; Schreiber et al. 2007), and CNG vehicles mainly emit nuclei-mode particles (Zhu et a., 2014; Toumasatos et al. (2020).   Zhu et al. (2014) calculated size-resolved particle emission factors from on-road diesel buses and CNG buses and reported that the PNSD of diesel buses dominate the accumulation mode diameters of 74-87 nm while the PNSD of CNG buses dominated the nucleation mode with modes at 21-24 nm. Total PN emissions of diesel buses per vehicle were 4 times higher than the level of CNG buses. However, the PN level in the nucleation mode (15-25 nm) of CNG buses was 1.7 times higher than from the diesel buses in the nucleation mode. Toumasatos et al. (2020) studied the particle emission performance of the Euro 6 CNG and gasoline vehicles and discussed the current EU cut-off solid PN size threshold of 23 nm. The results revealed that PN>23 nm represented 43 % of PN>10 nm and 8 % of PN>2.5 nm for gasoline vehicles and 7 % of PN>10 nm and 1 % of PN>2.5 nm for CNG vehicles respectively. These studies of emission PNSDs show that a significant number of particles reside below the EU lower measurement limit of of 23 nm, and many are even smaller than 10 nm. These probably contribute to the mode seen just appearing at the extreme small particle limit of Figure 9.

509   When the PNSD results measured in Delhi are compared with the main emission categories in the

510   literature (Kumar et al., 2013; Vu et al., 2015), it seems that the average size distributions measured

511   in the atmosphere in Delhi are much coarser, which is presumably due to condensation and

512   coagulation, or it could be that secondary particles dominate over the primary emissions. Pant et al.

513   (2016) hypothesised that the main accumulation mode peak in their winter measurements arose from

514   aqueous droplet evaporation, although this mechanism would be unlikely to explain the mode seen

515   in the summer data. Thamban et al. (2021) have also reported particle growth in the Delhi atmosphere

516   from condensation of organic compounds formed from oxidation processes.

517

518   Previous studies have attempted to quantify the relative contribution of primary and secondary

519   sources to the total and mode-segregated particle number concentrations (Kulmala et al. 2021;

520   Casquero-Vera et al. 2021; Hama et al. 2017; Kulmala et al. 2016; Rodríguez, & Cuevas, 2007).

521   Rodríguez and Cuevas (2007) first presented the methodology for the separation of traffic related

522   primary aerosol particles from the total using the BC as the main tracer of traffic. The method was

523   tested in this study, but did not prove appropriate as the BC sources in Delhi are more complex, and

524   arise not only from traffic. The BC diurnal trend (Figure 2) does not show the rush hour peaks, and

525   reflects mostly the combustion activity at night, presumably including the heavy duty diesel

526   emissions. A recent study by Kulmala et al. (2021) used NO_x as a tracer of primary sources. Figure 2

527   shows that only the NO_2 diurnal trend in autumn is clearly related to traffic sources. Furthermore the

528   sources of BC and NO_x are largely the same, as judged from the high similarity between BC and NO_x

529   diurnal trends (Figure 2).

530

531   **3.5   Correlations of PN with NO_2, NO, and BC**

532   Figure 10 shows the correlation coefficients between the hourly average PNs of five particle size

533   fractions and NO, NO_2, and BC measured in Delhi. Nucleation mode PN is better correlated with the

534   Aitken mode PN in winter and summer despite the lower correlation in autumn. The correlations

among >1 µm size fractions are higher in summer than winter and autumn. Tyagi et al. (2016) stated that the major source of NO_x emissions is vehicle exhaust and power plants in Delhi. Furthermore, studies have reported that approximately 80-90 % of NO_x and CO are produced from the transport sector in Delhi (Gurjar et al., 2004; Gulia et al., 2015; Tyagi et al., 2016; Hama et al., 2020). As seen in Figure 2, the NO_2 diurnal trend is very similar to nucleation and Aitken particle trends, especially in the autumn. NO_2 peaks in autumn in the traffic rush hours are larger than in winter and summer. In addition, there are no significant correlations between NO_2 and NO or BC in autumn (0.02 for NO, 0.03 for BC) compared to the summer (0.73 for NO, 0.61 for BC) and winter (0.37 for NO and 0.28 for BC) (Figure S12). NO and BC diurnal trends show the same higher level in the night (Figure 2) and also, they have higher correlation coefficients (0.78 in winter, 0.77 in summer, 0.72 in autumn) for all seasons, similar to the accumulation mode particle counts (Figure 2, Figure 10, Table S2). NO_2 and <100 nm particles may be associated with traffic sources, while the NO and BC and <1 µm particles could be associated with biomass burning, industry, (small generator) power generation, or possibly also with diesel vehicles.

3.6   Wind Effects

Figure S13 represents polar plots of BC, NO and NO_2 measured in Delhi. This shows no consistent pattern. There are differences between the pollutants in terms of directional and wind speed associations, and for each pollutant / season. There is no obvious indication of a strong local source influence, typically manifest as an intense area in the very centre of the plot circle. The plots for the particle size fractions (Figure 11) also show little consistency between seasons for a given size fraction. Within a season, however, adjacent size fractions often show a similarity of behaviour (consistent with their correlations, see above) but this similarity does not extend across all size ranges within a season.

4.   CONCLUSIONS

This study serves to highlight the remarkable complexity of airborne particulate matter in Delhi. The size distributions show marked seasonal changes, with coarse particles dominant in summer, but not in the cooler seasons, when the accumulation mode dominates. The measured size distributions show a fine mode aerosol with a considerably larger modal diameter than that typically seen in western countries, and larger than the modal emission size from major source categories. It appears the that the high particle concentrations and chemically reactive atmosphere are promoting rapid coagulation and condensational growth of particles, and therefore the measured size distributions are driven more by aerosol dynamical processes than source characteristics. Growth via a liquid droplet phase in the cooler months may also occur. There is little evidence for a contribution of new particle formation (although the summer season dataset is small), consistent with earlier work by Gani et al. (2020). Another notable feature is the apparent complexity and seasonal variability of sources of NO, NO_2 and BC, pollutants which can often be used to identify or locate sources of emissions. This is reflected in the various particle fractions, which generally correlate poorly with the other pollutants and with other than proximate size fractions.

The diurnal variation of all particle fractions is strongly suggestive of a road traffic influence, especially in the winter campaign. This appears strongly influenced by the emissions of heavy duty diesel traffic which is only able to access central Delhi at night. A size mode of <15 nm may well be attributable to vehicles using LPG/CNG fuels. However, the seasonal variability of the geographic distribution and wind speed dependence of sources revealed by the polar plots is strongly indicative of many other sources also contributing to all size fractions of particles.

DATA ACCESSIBILITY

Data supporting this publication are openly available from the UBIRA eData repository at

https://doi.org/10.25500/edata.bham.00000730

AUTHOR CONTRIBUTIONS

This study was conceived by RMH. WJB managed the research programme, and MSA and LRC collected the data. DCB and UAS led the data analysis with contributions from JB and DB. UAS and RMH co-authored the first draft. ZS and all co-authors provided comments and revisions.

COMPETING INTERESTS

The authors declare that they have no conflict of interest.

FINANCIAL SUPPORT

This research has been supported by the Natural Environment Research Council NE/P016499/1.

ACKNOWLEDGEMENTS

We are thankful the Scientific and Technical Research Council of Turkey (TUBITAK) (grant number 1059B191801445) to support the author Ulku Alver Sahin to work on the ASAP project. We would also like to acknowledgement the IIT Delhi team under the Principal Investigator-ship of Professor Mukesh Khare who provided all the facilities including space and logistical help during the experiment.

REFERENCES

Azimi, P., Zhao, D. and Stephens, B.: Estimates of HVAC filtration efficiency for fine and ultrafine particles of outdoor origin, Atmos. Environ., 98, 337-346, https://doi.org/10.1016/j.atmosenv.2014.09.007, 2014.

Babu, S. S., Manoj, M.R., Moorthy, K. K., Mukunda, M. G., Vijayakumar, S.N., Sobhan, K.K., Satheesh, S.K., Niranjan, K., Ramagopal, K., Bhuyan, P.K. and Singh, D.: Trends in aerosol optical depth over Indian region: Potential causes and impact indicators, J. Geophys. Res, 118, 11794–11806, https://doi.org/10.1002/2013JD020507, 2013.

Balakrishnan, K., Pillarisetti, A., Yamanashita, K. and Yusoff, K.: Air Pollution in Asia and the Pasific: Science Based Solution, Published by the United Nations Environment Programme (UNEP), Chapter 1.2 Air quality and health in Asia and the Pacific, January 2019, ISBN: 978-92-807-3725-7, Bangkok, Thailand, 2019.

Beddows, D. C. S., Dall'osto, M. and Harrison, R. M.: An Enhanced Procedure for the Merging of Atmospheric Particle Size Distribution Data Measured Using Electrical Mobility and Time-of-Flight Analysers, Aerosol Science and Technology, 44, 11, 930-938, https://doi.org/10.1080/02786826.2010.502159, 2010.

Bhandari, S., Gani, S., Patel, K., Wang, D. S., Soni, P., Arub, Z., Habib, G., Apte, J.S. and Ruiz, L. H.: Sources and atmospheric dynamics of organic aerosol in New Delhi, India: insights from receptor modeling, Atmos. Chem. Phys., 20, 735–752, https://doi.org/10.5194/acp-20-735-2020, 2020.

Bikkina, S., Andersson, A., Kirillova, E. N., Holmstrand, H., Tiwari, S., Srivastava, A. K., Bisht, D.S. and Gustafsson, Ö.: Air quality in megacity Delhi affected by countryside biomass burning, Nature Sustainability, 2, 200–205, https://doi.org/10.1038/s41893-019-0219-0, 2019.

Bousiotis, D., Dall'Osto, M., Beddows, D. C. S., Pope, F. D., and Harrison, R. M.: Analysis of new particle formation (NPF) events at nearby rural, urban background and urban roadside sites, Atmos. Chem. Phys., 19, 5679–5694, https://doi.org/10.5194/acp-19-5679-2019, 2019.

Bousiotis, D., Brean, J., Pope, F. D., Dall'Osto, M., Querol, X., Alastuey, A., Perez, N., Petäjä, T., Massling, A., Nøjgaard, J. K., Nordstrøm, C., Kouvarakis, G., Vratolis, S., Eleftheriadis, K., Niemi, J. V., Portin, H., Wiedensohler, A., Weinhold, K., Merkel, M., Tuch, T., and Harrison, R. M.: The effect of meteorological conditions and atmospheric composition in the occurrence and development of new particle formation (NPF) events in Europe, Atmos. Chem. Phys., 21, 3345–3370, https://doi.org/10.5194/acp-21-3345-2021, 2021.

Butt, E. W., Rap, A., Schmidt, A., Scott, C. E., Pringle, K. J., Reddington, C. L., Richards, N. A. D., Woodhouse, M. T., Ramirez-Villegas, J., Yang, H., Vakkari, V., Stone, E. A., Rupakheti, M., S. Praveen, P., G. van Zyl, P., P. Beukes, J., Josipovic, M., Mitchell, E. J. S., Sallu, S. M., Forster, P. M., and Spracklen, D. V.: The impact of residential combustion emissions on atmospheric aerosol, human health, and climate, Atmos. Chem. Phys., 16, 873–905, https://doi.org/10.5194/acp-16-873-2016, 2016.

Casquero-Vera, J. A., Lyamani, H., Titos, G., Minguillón, M. C., Dada, L., Alastuey, A., Querol, X., Petäjä, T., Olmo, F. J. and Alados-Arboledas, L.: Quantifying traffic, biomass burning and secondary source contributions to atmospheric particle number concentrations at urban and

suburban sites, Science of The Total Environment, 768, 145282, doi.org/10.1016/j.scitotenv.2021.145282, 2021.

Chelani, A. B., Gajghate, D. G., ChalapatiRao, C. V. and Devotta, S.: Particle Size Distribution in Ambient Air of Delhi and Its Statistical Analysis, Bull. Environ. Contam. Toxicol., 85, 22–27, https://doi.org/10.1007/s00128-010-0010-4, 2010.

Chen, F., Zhang, X., Zhu, X., Zhang, H., Gao, J. and Hopke, P. K.: Chemical Characteristics of PM2.5 during a 2016 Winter Haze Episode in Shijiazhuang, China. Aerosol Air Qual. Res., 17, 368-380, https://doi.org/10.4209/aaqr.2016.06.0274, 2017.

Chowdhury, S., Dey, S., Tripathi, S. N., Beig, G., Mishra, A. K. and Sharma, S.:” Traffic intervention” policy fails to mitigate air pollution in megacity Delhi, Environmental Science & Policy, 74, 8-13, https://doi.org/10.1016/j.envsci.2017.04.018, 2017.

Conibear, L., Butt, E. W., Knote, C., Arnold, S. R. and Spracklen, D. V.: Residential energy use emissions dominate health impacts from exposure to ambient particulate matter in Indi,. Nat. Commun., 9, 617, https://doi.org/10.1038/s41467-018-02986-7, 2018.

Cusworth, D. H., Mickley, L. J., Sulprizio, M. P., Liu, T., Marlier, M.E., DeFries, R. S., Guttikunda, S.K. and Gupta, P.: Quantifying the influence of agricultural fires in northwest India on urban air pollution in Delhi, India, Environ. Res. Lett., 13, 044018, https://doi.org/10.1088/1748-9326/aab303, 2018.

Dal Maso, M., Kulmala, M., Riipinen, I., Wagner, R., Hussein, T., Aalto, P. P. and Lehtinen, K. E. J.: Formation and growth of fresh atmospheric aerosols: eight years of aerosol size distribution data from SMEAR II, Hyytiala, Finland, Boreal Environmental Research 10, 323-336, 2005.

Dandona, L., Dandona, R., Kumar, G. A., Shukla, D. K., Paul, V. K., Balakrishnan, K., Prabhakaran, D., Tandon, N., Salvi, S., Dash, A. P., Nandakumar, A., Patel, V., Agarwal, S. K., Gupta, P. C., Dhaliwal, R. S., Mathur, P., Laxmaiah, A., Dhillon, P. K., Dey, S., Mathur, M. R., Afshin, A., Fitzmaurice, C., Gakidou, E., Gething, P., Hay, S.I., Kassebaum, N. J., Kyu, H., Lim, S. S., Naghavi, M., Roth, G. A., Stanaway, J. D., Whiteford, H., Chadha, V. K., Khaparde, S. D., Rao, R., Rade, K., Dewan, P., Furtado, M., Dutta, E., Varghese, C. M., Mehrotra, R., Jambulingam, P., Kaur, T., Sharma, M., Singh, S., Arora, R., Rasaily, R., Anjana, R. M., Mohan, V., Agrawal, A., Chopra, A., Mathew, A. J., Bhardwaj, D., Muraleedharan, P., Mutreja, P., Bienhoff, K., Glenn, S., Abdulkader, R. S., Aggarwal, A. N., Aggarwal, R., Albert, S., Ambekar, A., Arora, M., Bachani, D., Bavdekar, A., Beig, G., Bhansali, A., Bhargava, A., Bhatia, E., Camara, B., Christopher, D. J., Das, S. K., Dave, P. V., Dey, S., Ghoshal, A. G., Gopalakrishnan, N., Guleria, R., Gupta, R., Gupta, S. S., Gupta, T., Gupte, M. D., Gururaj, G., Harikrishnan, S., Iyer, V., Jain, S.K., Jeemon, P., Joshua, V., Kant, R., Kar, A., Kataki, A.C., Katoch, K., Khera, A., Kinra, S., Koul, P.A., Krishnan, A., Kumar, A., Kumar, R. K., Kumar, R., Kurpad, A., Ladusingh, L., Lodha, R., Mahesh, P. A., Malhotra, R., Mathai, M., Mavalankar, D., Mohan Bv, M., Mukhopadhyay, S., Murhekar, M., Murthy, G.V.S., Nair, S., Nair, S. A., Nanda, L., Nongmaithem, R. S., Oommen, A.M., Pandian, J.D., Pandya, S., Parameswaran, S., Pati, S., Prasad, K., Prasad, N., Purwar, M., Rahim, A., Raju, S., Ramji, S., Rangaswamy, T., Rath, G. K., Roy, A., Sabde, Y., Sachdeva, K. S., Sadhu, H., Sagar, R., Sankar, M. J., Sharma, R., Shet, A., Shirude, S., Shukla, R., Shukla, S. R., Singh, G., Singh, N. P., Singh, V., Sinha, A., Sinha, D. N., Srivastava, R. K., Srividya, A., Suri, V., Swaminathan, R., Sylaja, P. N., Tandale, B., Thakur, J. S., Thankappan, K.R., Thomas, N., Tripathy, S., Varghese, M., Varughese, S., Venkatesh, S., Venugopal, K., Vijayakumar, L., Xavier, D., Yajnik, C. S., Zachariah, G., Zodpey, S., Rao, J. V. R. P., Vos, T., Reddy, K. S., Murray, C. J. L. and Swaminathan, S.: Nations within a nation: variations in epidemiological transition across the states

of India, 1990-2016 in the global burden of disease study. The Lancet, 390, 10111, 2437-2460, https://doi.org/10.1016/S0140-6736(17)32804-0, 2017.

Das, A., Kumar, A., Habib, G. and Vivekanandan, P.: Insights on the biological role of ultrafine particles of size PM<0.25: A prospective study from New Delhi, Environmental Pollution, 268, Part B, 115638, https://doi.org/10.1016/j.envpol.2020.115638, 2021.

DeCarlo, P. F., Slowik, J. G., Worsnop, D. R., Davidovits, P. and Jimenez, J. L.: Particle Morphology and Density Characterization by Combined Mobility and Aerodynamic Diameter Measurements. Part 1: Theory, Aerosol Science and Technology, 38:12, 1185-1205, https://doi.org/10.1080/027868290903907, 2004.

Dhyani, R., Sharma, N. and Advani, M.: Estimation of Fuel Loss and Spatial-Temporal Dispersion of Vehicular Pollutants at a Signalized Intersection in Delhi City, India. WIT Transection on Ecology and the Environmen: Air Pollution 2019, WIT Press, 236, 233-247, ISBN: 978-1-78466-343-8, Editor: Passerini et al., 2019.

Dumka, U. C., Tiwari, S., Kaskaoutis, D. G., Soni, V. K., Safai, P. D. and Attri, S. D.: Aerosol and pollutant characteristics in Delhi during a winter research campaign, Environ. Sci. Pollut. Res., 26, 3771–3794. https://doi.org/10.1007/s11356-018-3885-y, 2019.

Gani S., Bhandari, S., Patel, K., Seraj, S., Soni, P., Arub, Z., Habib, G., Ruiz, L.H. and Apte, J.S.: Particle number concentrations and size distribution in a polluted megacity: the Delhi Aerosol Supersite study, Atmos. Chem. Phys., 20, 8533–8549, https://doi.org/10.5194/acp-20-8533-2020, 2020.

Giechaskiel, B., Lähde, T. and Drossinos, Y. Regulating particle number measurements from the tailpipe of light-duty vehicles: The next step?, Environmental Research, 172, 1-9, https://doi.org/10.1016/j.envres.2019.02.006, 2019.

Gulia, S., Shiva Nagendra, S.M., Khare, M. and Khanna, I.: Urban air quality management-A review, Atmospheric Pollution Research, 6, 2, 286-304, https://doi.org/10.5094/APR.2015.033, 2015.

Guo, H., Kota, S.H., Sahu, S.K., Hu, J., Ying, Q., Gao, A. and Zhang, H.: Source apportionment of PM2.5 in North India using source-oriented air quality models, Environmental Pollution, 231, 1, 426-436, https://doi.org/10.1016/j.envpol.2017.08.016, 2017.

Gupta, S., Kumar, K., Srivastava, A., Srivastava, A. and Jain, V. K.: Size distribution and source apportionment of polycyclic aromatic hydrocarbons (PAHs) in aerosol particle samples from the atmospheric environment of Delhi, India, Science of The Total Environment, 409, 22, 4674-4680, https://doi.org/10.1016/j.scitotenv.2011.08.008., 2011.

Gurjar, B. R., van Aardenne, J. A., Lelieveld, J. and Mohan, M.: Emission estimates and trends (1990–2000) for megacity Delhi and implications, Atmospheric Environment, 38, 33, 5663-5681, https://doi.org/10.1016/j.atmosenv.2004.05.057, 2004.

Guttikunda, S. K., Goel, R. and Pant, P.: Nature of air pollution, emission sources, and management in the Indian cities, Atmospheric Environment, 95, 501-510, https://doi.org/10.1016/j.atmosenv.2014.07.006, 2014.

Guttikunda, S.K. and Gurjar, B.R.: Role of meteorology in seasonality of air pollution in megacity Delhi, India, Environ. Monit. Assess., 184, 3199–3211. https://doi.org/10.1007/s10661-011-2182-8, 2012.

Hama, S.M.L., Kumar, P., Harrison, R.M., Bloss, W.J., Khare, M., Mishra, S., Namdeo, A., Sokhi, R., Goodman, P. and Sharma, C.: Four-year assessment of ambient particulate matter and trace gases in the Delhi-NCR region of India, Sustainable Cities and Society, 54, 102003, https://doi.org/10.1016/j.scs.2019.102003, 2020.

Hama, S.M.L., Cordell, R. L. and Monks, P. S.: Quantifying primary and secondary source contributions to ultrafine particles in the UK urban background, Atmos. Environ., 166, 62-78, doi.org/10.1016/j.atmosenv.2017.07.013, 2017.

Hamed, A., Joutsensaari, J., Mikkonen, S., Sogacheva, L., Dal Maso, M., Kulmala, M., Cavalli, F., Fuzzi, S., Facchini, M. C., Decesari, S., Mircea, M., Lehtinen, K. E. J., and Laaksonen, A.: Nucleation and growth of new particles in Po Valley, Italy, Atmos. Chem. Phys., 7, 355–376, https://doi.org/10.5194/acp-7-355-2007, 2007.

Han, Y., Iwamoto, Y., Nakayama, T., Kawamura, K., Hussein, T. and Mochida, M.: Observation of new particle formation over a mid-latitude forest facing the North Pacific, Atmos. Environ., 64, 77-84, https://doi.org/10.1016/j.atmosenv.2012.09.036, 2013.

Harrison RM.: Airborne particulate matter, Phil. Trans. R. Soc. A, 378, 20190319. http://dx.doi.org/10.1098/rsta.2019.0319, 2020.

Harrison, R. M., Rob MacKenzie, A., Xu, H., Alam, M. S., Nikolova, I., Zhong, J., ... and Liang, Z., Diesel exhaust nanoparticles and their behaviour in the atmosphere. Proceedings of the Royal Society A, 474(2220), 20180492, 2018.

Harrison, R. M., Beddows, D.C.S. and Dall'Osto, M.: PMF Analysis of Wide-Range Particle Size Spectra Collected on a Major Highway, Environ. Sci. Technol., 45, 13, 5522–5528, https://doi.org/10.1021/es2006622, 2011.

Jain, S., Sharma, S. K., Vijayan, N., Mandal, T. K.: Seasonal characteristics of aerosols (PM2.5 and PM10) and their source apportionment using PMF: A four year study over Delhi, India, Environmental Pollution, 262, 114337, https://doi.org/10.1016/j.envpol.2020.114337, 2020.

Jeong, C.H., Evans, G. J., McGuire, M. L., Chang, R. Y.W. and Abbatt, J. P. D.: Zeromskiene, K., Mozurkewich, M., Li, S.-M., and Leaitch, W. R.: Particle formation and growth at five rural and urban sites, Atmos. Chem. Phys., 10, 7979–7995, https://doi.org/10.5194/acp-10-7979-2010, 2010.

Jing, H., Li, Y.F., Zhao, J., Li, B., Sun, J., Chen, R., Gao, Y. and Chen, C.: Wide-range particle characterization and elemental concentration in Beijing aerosol during the 2013 Spring Festival, Environmental Pollution, 192, 204-211, https://doi.org/10.1016/j.envpol.2014.06.003, 2014.

Kalafut-Pettibone, A. J., Wang, J., Eichinger, W. E., Clarke, A., Vay, S. A., Blake, D. R., and Stanier, C. O.: Size-resolved aerosol emission factors and new particle formation/growth activity occurring in Mexico City during the MILAGRO 2006 Campaign, Atmos. Chem. Phys., 11, 8861–8881, https://doi.org/10.5194/acp-11-8861-2011, 2011.

808 Kanawade, V.P., Srivastava, A.K., Ram, K., Asmi, E., Vakkari, V., Soni, V.K., Varaprasad, V. and
809 Sarangi, C.: What caused severe air pollution episode of November 2016 in New Delhi?, Atmos.
810 Environ., 222, 117125, https://doi.org/10.1016/j.atmosenv.2019.117125, 2020.

812 Kontses, A., Triantafyllopoulos, G., Ntziachristos, L. and Samaras, Z.: Particle number (PN)
813 emissions from gasoline, diesel, LPG, CNG and hybrid-electric light-duty vehicles under real-world
814 driving conditions, Atmos. Environ., 222, 117126, https://doi.org/10.1016/j.atmosenv.2019.117126,
815 2020.

817 Kuang, C., Chen, M., Zhao, J., Smith, J., McMurry, P. H., and Wang, J.: Size and time-resolved
818 growth rate measurements of 1 to 5 nm freshly formed atmospheric nuclei, Atmos. Chem. Phys.,
819 12, 3573–3589, https://doi.org/10.5194/acp-12-3573-2012, 2012.

821 Kulmala, M., Dada, L., Daellenbach, K.r., Yan, C., Stolzenburg, D., Kontkanen, J., Ezhova, E.,
822 Hakala, S., Tuovinen, S., Kokkonen, T.V., Kurpp, M., Cai, R., Zhou, Y., Yin, R., Baalbaki, R.,
823 Chan, T., Chu, B., Deng, C., Fu, Y., Ge, M., He, H., Heikkinen, L., Junninen, H., Liu, Y., Lu, Y.,
824 Nie, W., Rusanen, A., Vakkari,V., Wang, Y., Yang, G., Yao, L., Zheng, J., Kujansuu, J.,
825 Kangasluoma, J., Petäjä, T., Paasonen, P., Järvi, L., Worsnop, D., Ding, A., Liu, Y., Wang, L.,
826 Jiang, J., Bianchi, F. and Kerminen, V.M.: Is reducing new particle formation a plausible solution to
827 mitigate particulate air pollution in Beijing and other Chinese megacities? Faraday Discussion 226,
828 221, doi.org/10.1039/D0FD00078G, 2021.

830 Kulmala M., Luoma K., Virkkula A., Petäjä T., Paasonen P., Kerminen V.-M., Nie W., Qi X., Shen
831 Y., Chi X. and Ding A.: On the mode-segregated aerosol particle number concentration load:
832 contributions of primary and secondary particles in Hyytiälä and Nanjing. Boreal, Env. Res., 21,
833 319–331. 2016.

835 Kumar, A., Ambade, B., Sankar, T. K., Sethi, S. S. and Kurwadkar, S.: Source identification and
836 health risk assessment of atmospheric PM2.5-bound polycyclic aromatic hydrocarbons in
837 Jamshedpur, India, Sustainable Cities and Society, 52, 101801,
838 https://doi.org/10.1016/j.scs.2019.101801, 2020.

840 Kumar, P., Gulia, S., Harrison, R. M. and Khare, M.: The influence of odd–even car trial on fine
841 and coarse particles in Delhi, Environmental Pollution, 225, 20-30,
842 https://doi.org/10.1016/j.envpol.2017.03.017, 2017.

844 Kumar, P., Pirjola, L., Ketzel, M., and Harrison, R. M.: Nanoparticle emissions from 11 non-
845 vehicle exhaust sources – A review, Atmos. Environ., 67, 252–277,
846 https://doi.org/10.1016/j.atmosenv.2012.11.011, 2013.

848 Iida, K., Stolzenburg, M.R., McMurry, P.H. and Smith, J.N.: Estimating nanoparticle growth rates
849 from size-dependent charged fractions: Analysis of new particle formation events in Mexico City,
850 J. Geophys. Res., 113, D05207, doi.org/10.1029/2007JD009260, 2008

852 Liu, J., Jiang, J., Zhang, Q., Deng, J., and Hao, J.: A spectrometer for measuring particle size
853 distributions in the range of 3 nm to 10 μm, Front. Environ. Sci. Eng., 10, 63–72,
854 https://doi.org/10.1007/s11783-014-0754-x, 2016.

856 Magara-Gomez, K.T., Olson, M.R., McGinnis, J.E., Zhang, M. and Schauer, J.J.: Effect of Ambient
857 Temperature and Fuel on Particle Number Emissions on Light-Duty Spark-Ignition Vehicles,
858 Aerosol Air Qual. Res., 14, 1360-1371. https://doi.org/10.4209/aaqr.2013.06.0183, 2014.
859

Mahato, S., Pal, S. and Ghosh, K. G.: Effect of lockdown amid COVID-19 pandemic on air quality of the megacity Delhi, India, Science of The Total Environment, 730, 139086, https://doi.org/10.1016/j.scitotenv.2020.139086, 2020.

Masiol, M., Vu, T. V., Beddows, D. C. S. and Harrison, R. M.: Source apportionment of wide range particle size spectra and black carbon collected at the airport of Venice (Italy), Atmospheric Environment, 139, 56-74, https://doi.org/10.1016/j.atmosenv.2016.05.018, 2016.

Mönkkönen, P., Koponen, I. K., Lehtinen, K. E. J., Hämeri, K., Uma, R., and Kulmala, M.: Measurements in a highly polluted Asian mega city: observations of aerosol number size distribution, modal parameters and nucleation events, Atmos. Chem. Phys., 5, 57–66, https://doi.org/10.5194/acp-5-57-2005, 2005.

Nagpure, A.S., Ramaswami, A. and Russell, A.: Characterizing the Spatial and Temporal Patterns of Open Burning of Municipal Solid Waste (MSW) in Indian Cities, Environ. Sci. Technol., 49, 21, 12904–12912, https://doi.org/10.1021/acs.est.5b03243, 2015.

Narain, U. and Krupnick, A., The Impact of Delhi's CNG Program on Air Quality. RFF Discussion Paper No. 07-06, Available at SSRN: https://ssrn.com/abstract=969727 or http://dx.doi.org/10.2139/ssrn.969727, 2007.

Ondráček, J., Ždímal, V., Smolík, J., and Lazaridis, M.: A Merging Algorithm for Aerosol Size Distribution from Multiple Instruments, Water Air Soil Pollut., 199, 219–233, https://doi.org/10.1007/s11270-008-9873-y, 2009.

Pant, P. and Harrison, R. M.: Critical Review of Receptor Modelling for Particulate Matter: A Case Study of India, Atmos. Environ., 49, 1-12, https://doi.org/10.1016/j.atmosenv.2011.11.060, 2012.

Pant, P., Baker, S. J., Goel, R., Guttikunda, S., Goel, A., Shukla, A. and Harrison, R.M.: Analysis of size-segregated winter season aerosol data from New Delhi, India, Atmos. Poll. Res., 7, 1, 100-109, https://doi.org/10.1016/j.apr.2015.08.001., 2016.

R Core Team, 2015. R: a Language and Environment for Statistical Computing. R Foundation for Statistical Computing, Vienna, Austria. http://www.R-project.org/.

Rai, P., Furger, M., Haddad, I.E., Kumar, V., Wang, L., Singh, A., Dixit, K., Bhattu, D., Petit, J.E., Ganguly, D., Rastogi, N., Baltensperger, U., Tripathi, S.N., Slowik, J.G. and Prévôt, A.S.H.: Real-time measurement and source apportionment of elements in Delhi's atmosphere, Science of The Total Environment, 742, 140332, https://doi.org/10.1016/j.scitotenv.2020.140332, 2020.

Rodríguez, S. and Cuevas, E.: The contributions of "minimum primary emissions" and "new particle formation enhancements" to the particle number concentration in urban air, Journal of Aerosol Science 38, 1207-1219, https://doi.org/10.1016/j.jaerosci.2007.09.001, 2007.

Rodríguez-Urrego, D. and Rodríguez-Urrego, L.: Air quality during the COVID-19: PM2.5 analysis in the 50 most polluted capital cities in the world, Environmental Pollution, 266, 1, 115042, https://doi.org/10.1016/j.envpol.2020.115042, 2020.

Salvador, P., Barreiro, M., Gómez-Moreno, F. J., Alonso-Blanco, E. and Artíñano, B.: Synoptic classification of meteorological patterns and their impact on air pollution episodes and new particle formation processes in a south European air basin, Atmos.c Environ., 245, 118016, https://doi.org/10.1016/j.atmosenv.2020.118016, 2021.

Sarangi, B., Aggarwal, S. G., and Gupta, P. K.: A simplified approach to calculate particle growth rate due to self-coagulation, scavenging and condensation using SMPS measurements during a particle growth event in New Delhi, Aerosol and air quality research, 15(1), 166-179, https://doi: 10.4209/aaqr.2013.12.0350, 2015.

Sarangi, B., Aggarwal, S. G., Kunwar, B., Kumar, S., Kaur, R., Sinha, D., Tiwari, S. and Kawamura, K.: Nighttime particle growth observed during spring in New Delhi: Evidences for the aqueous phase oxidation of SO2, Atmospheric environment, 188, 82-96, https://doi.org/10.1016/j.atmosenv.2018.06.018, 2018

Schmid, O., Karg, E., Hagen, D. E., Whitefield, P. D. and Ferron, G. A.: On the Effective Density of Non-Spherical Particles as Derived From Combined Measurements of Aerodynamic and Mobility Equivalent Size, Atmos. Environ., 38, 431–443. https://doi.org/10.1016/j.jaerosci.2007.01.002, 2007.

Schreiber, D., Forss, A. M., Mohr, M. and Dimopoulos, P.: Particle Characterisation of Modern CNG, Gasoline and Diesel Passenger Cars, 8th International Conference on Engines for Automobiles, Technical Paper 2007-24-0123, ISSN: 0148-7191, e-ISSN: 2688-3627, https://doi.org/10.4271/2007-24-0123, 2007.

Tiwari, S., Bisht, D.S., Srivastava, A.K., Pipal, A.S., Taneja, A., Srivastava, M.K. and Attri, S.D.: Variability in atmospheric particulates and meteorological effects on their mass concentrations over Delhi, India, Atmospheric Research, 145–146, 45-56, https://doi.org/10.1016/j.atmosres.2014.03.027, 2014.

Thamban, N.M., Lalchandani, V., Kumar, V., Mishra, S., Bhattu, D., Slowik, J.G., Prevot, A.S.H., Satish, R., Rastogi, N., Tripathi, S.N.: Evolution of size and composition of fine particulate matter in the Delhi megacity during later winter, Atmospheric Environment, 267,118752, doi.org/10.1016/j.atmosenv.2021.118752. 2021.

Toumasatos, Z., Kontses, A., Doulgeris, S., Samaras, Z. and Ntziachristos, L.: Particle emissions measurements on CNG vehicles focusing on Sub-23nm, Aerosol Science and Technology, 55, 2, 182-193, https://doi.org/10.1080/02786826.2020.1830942, 2021.

Tyagi, S., Tiwari, S., Mishra, A., Hopke, P.K., Attri, S.D., Srivastava, A.K. and Bisht, D. S.: Spatial variability of concentrations of gaseous pollutants across the National Capital Region of Delhi, India, Atmospheric Pollution Research, 7, 5, 808-816, https://doi.org/10.1016/j.apr.2016.04.008, 2016.

Vu, T. V., Delgado-Saborit, J. M. and Harrison, R. M.: Particle number size distributions from seven major sources and implications for source apportionment studies. Atmospheric Environment, 122, 114-132, https://doi.org/10.1016/j.atmosenv.2015.09.027, 2015.
Wu, T. and Boor, B. E.: Urban aerosol size distributions: a global perspective, Atmos. Chem. Phys., 21, 8883–8914, https://doi.org/10.5194/acp-21-8883-2021, 2021.

Yadav, R., Sahu, L.K., Beig, G. and Jaaffrey, S.N.A.: Role of long-range transport and local meteorology in seasonal variation of surface ozone and its precursors at an urban site in India, Atmospheric Research, 176–177, 96-107,https://doi.org/10.1016/j.atmosres.2016.02.018, 2016.

Zhang, Y. M., Zhang, X. Y., Sun, J. Y., Lin, W. L., Gong, S. L., Shen, X. J. and Yang, S.: Characterization of new particle and secondary aerosol formation during summertime in Beijing,

963 China, Tellus B: Chemical and Physical Meteorology, 63:3, 382-394,

964 https://doi.org/10.1111/j.1600-0889.2011.00533.x, 2011.

965

966 Zhu, C., Li, J.G., Wang, L., Morawska, L., Zhang, X. and Zhang, Y.L.: Size-resolved particle

967 distribution and gaseous concentrations by real-world road tunnel measurement, Indoor and Built

968 Environment, 23, 2, 225-235, https://doi.org/10.1177/1420326X13509290, 2014.

FIGURE CAPTIONS:

Figure 1. Comparison of average particle number counts (#/cm^3) for nucleation, aitken, accumulation, large fine and coarse modes of PM between 15 nm and 10 µm in all seasons, and the volume contributions for comparison.

Figure 2. Average diurnal variation of particle number counts for nucleation, Aitken, accumulation, large fine and coarse modes and PM$_{2.5}$, BC, NO and NO$_2$ in autumn, summer and winter.

Figure 3. Average diurnal variation of total particle number counts (between 15 and 10 µm) for weekday average (Monday to Friday), Saturday and Sunday in Delhi. (Summer data are very limited. There are no data on Friday afternoon, night and Saturday early morning (Figure S6)).

Figure 4. Diurnal contour plots for particles derived by SMPS between 15 and 660 nm averaged for each season (a: winter, b: Autumn and c: Summer) and for 3 June 2018 data when a NPF event probably occurred (d), the solid line showing the NO$_x$ mixing ratio. Note the different scales for the seasons presented.

Figure 5. The hourly average of day and night particle numbers for all modes from the wide range particle sizes derived from the merged data. UFP = Nucleation +Aitken, PN$_1$ = UFP+Accumulation, PN$_{10}$ = PN$_1$+Large Fine+Coarse.

Figure 6. Seasonal average (line) and standard deviation (shadow) of particle number size distributions.

Figure 7. Hourly average day and night (left side) and during day hours (right side) particle number distributions in autumn, summer and winter in Delhi.

Figure 8. Diurnal change of the geometric mean diameter (GMD) calculated for winter, autumn and summer seasons. Growth rates (nm/hour) are calculated from dGMD/dt.

Figure 9. Hourly average particle number, volume and area distributions in the winter (a), autumn (b) and summer (c) in Delhi.

Figure 10. Correlation coefficient (R) between the hourly average PNs of five particle size fractions (left side) and NO, NO$_2$, BC (right side).

Figure 11. Polar plots of PNs (#/cm^3) for five particle size fractions in winter, autumn and summer in Delhi.

1013

1014

1015

1016

1017 **Figure 1.** Comparison of average particle number counts (#/cm^3) for nucleation, aitken,
1018 accumulation, large fine and coarse modes of PM between 15 nm and 10 µm in all seasons, and the
1019 volume contributions for comparison.
1020
1021

1022
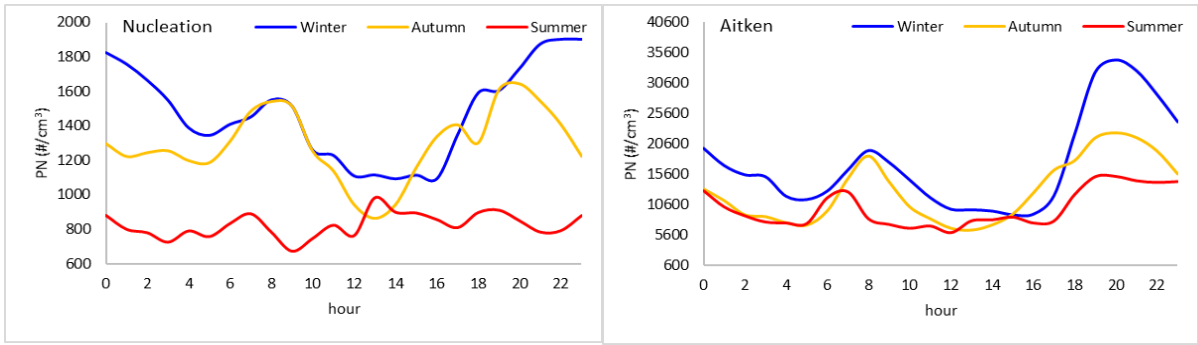
1023
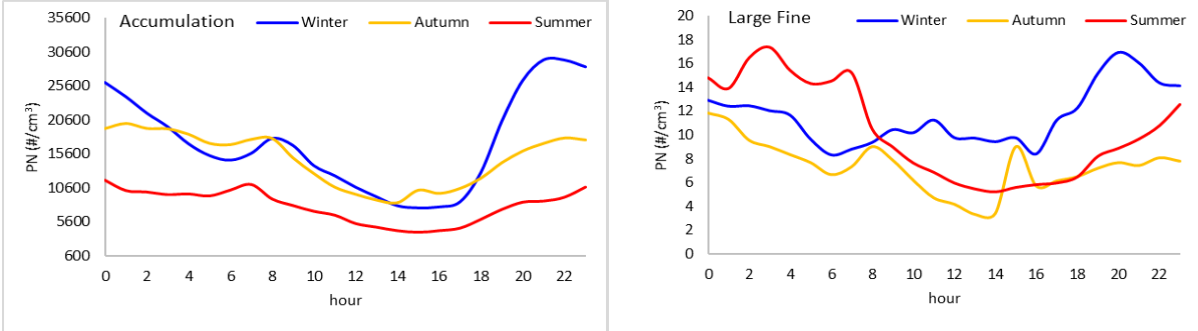
1024
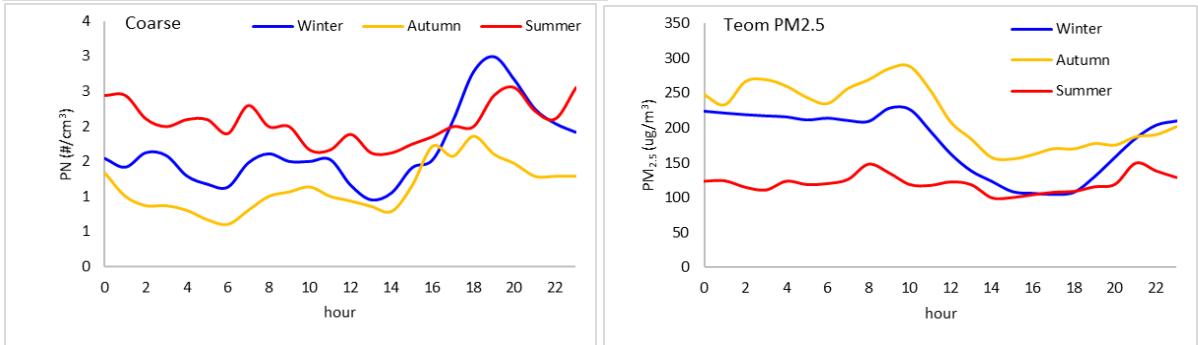
1025
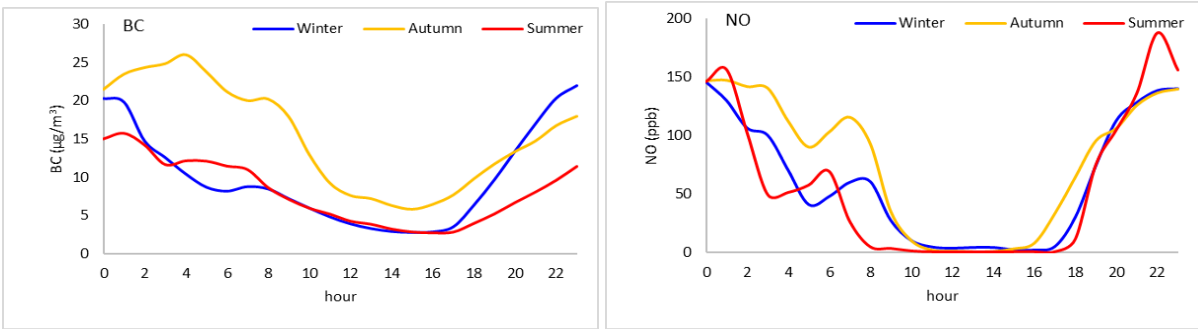
1026
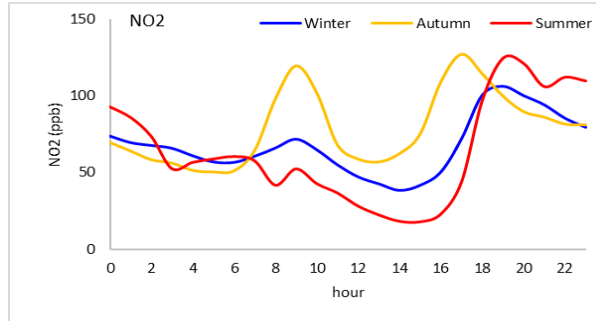
Figure 2. Average diurnal variation of particle number counts for nucleation, Aitken, accumulation, large fine and coarse modes and $PM_{2.5}$, BC, NO and NO_2 in autumn, summer and winter.

1027
1028
1029
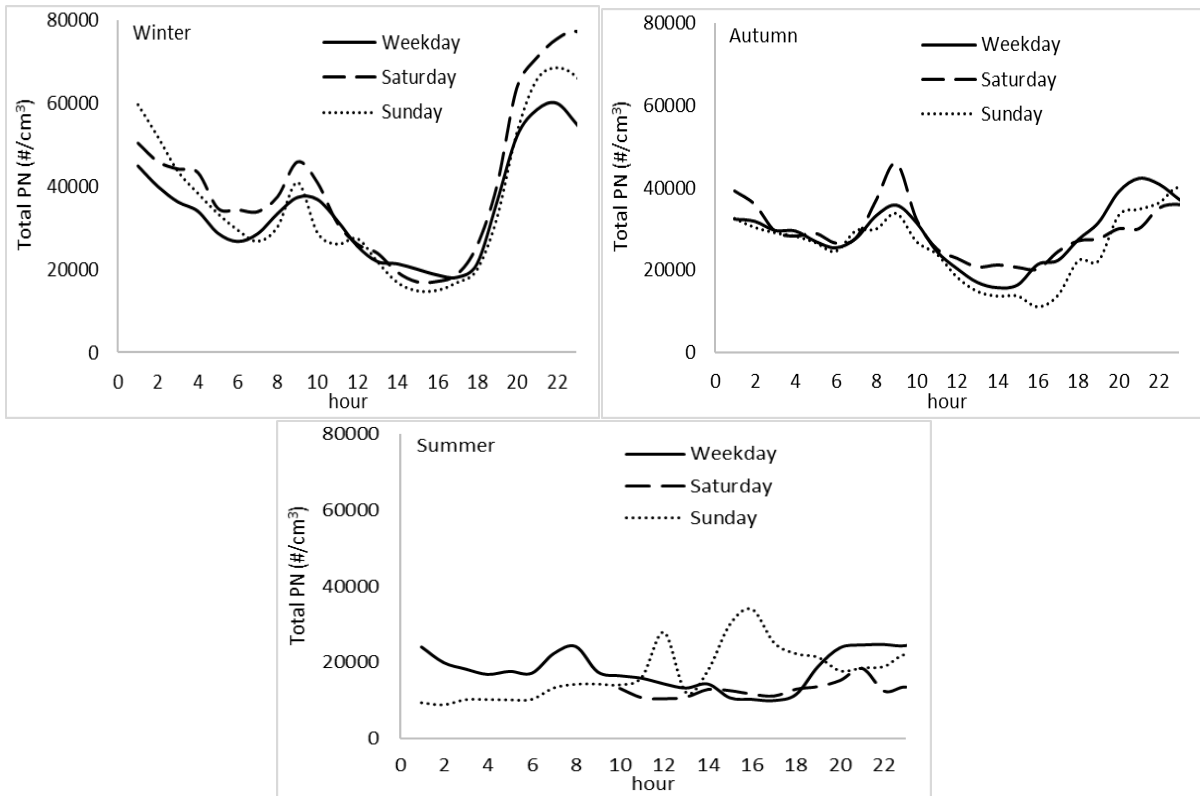
Figure 3. Average diurnal variation of total particle number counts (between 15 and 10 µm) for weekday average (Monday to Friday), Saturday and Sunday in Delhi. (Summer data are very limited. There are no data on Friday afternoon, night and Saturday early morning (Figure S6)).

1037
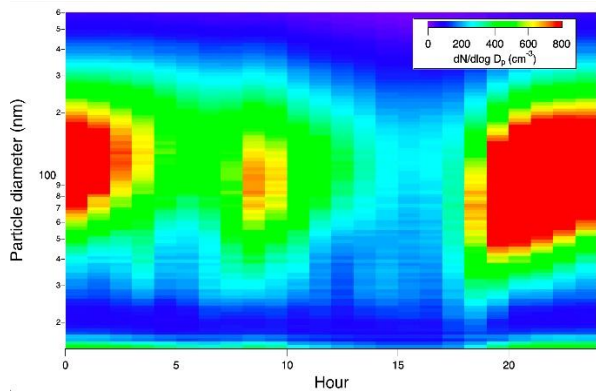
1038   a)   Winter   b) Autumn
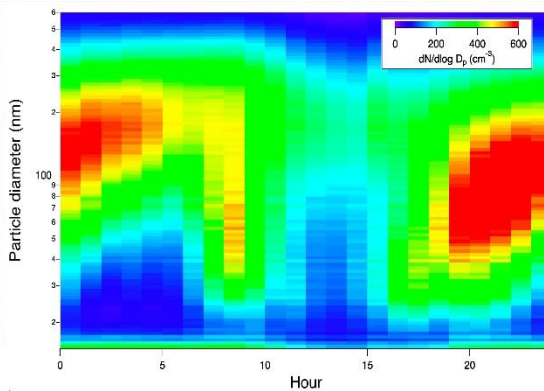
1039
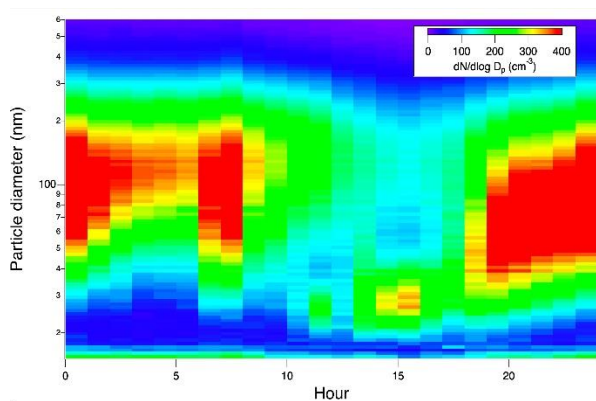
1040   c)   Summer   d) 3 June 2018

1041
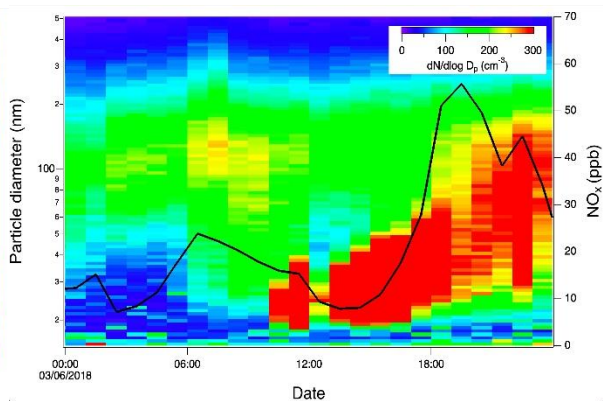
1042 **Figure 4.** Diurnal contour plots for particles derived by SMPS between 15 and 660 nm averaged for
1043 each season (a: winter, b: Autumn and c: Summer) and for 3 June 2018 data when a NPF event
1044 probably occurred (d), the solid line showing the NO_x mixing ratio. Note the different scales for the
1045 seasons presented.

1046
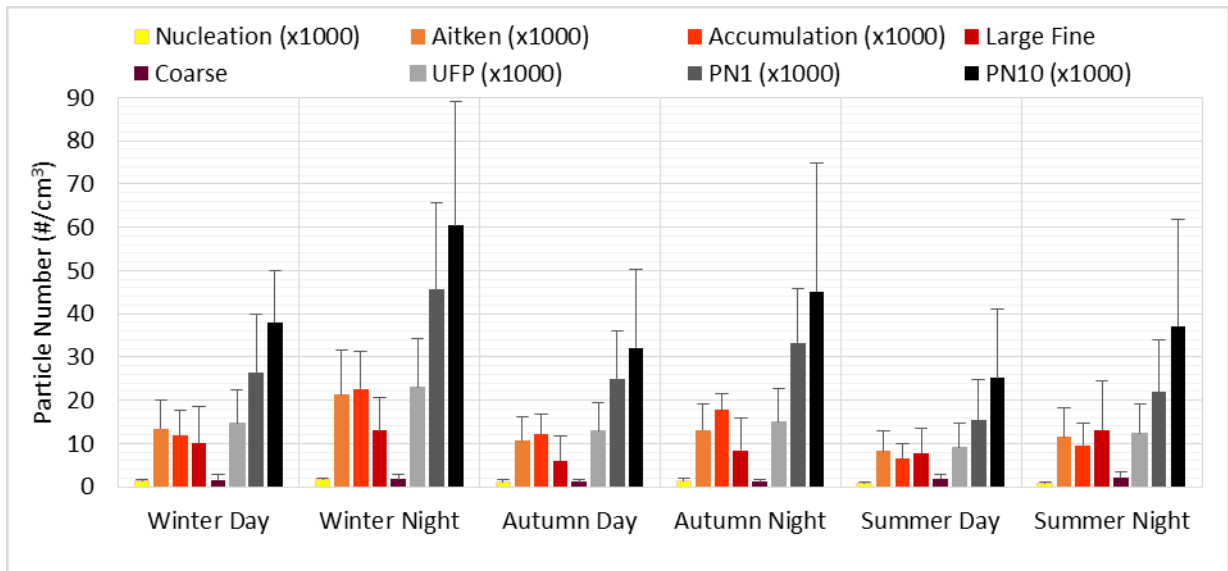
Figure 5. The hourly average of day and night particle numbers for all modes from the wide range particle sizes derived from the merged data. UFP = Nucleation +Aitken, PN_1 = UFP+Accumulation, PN_{10} = PN_1+Large Fine+Coarse.
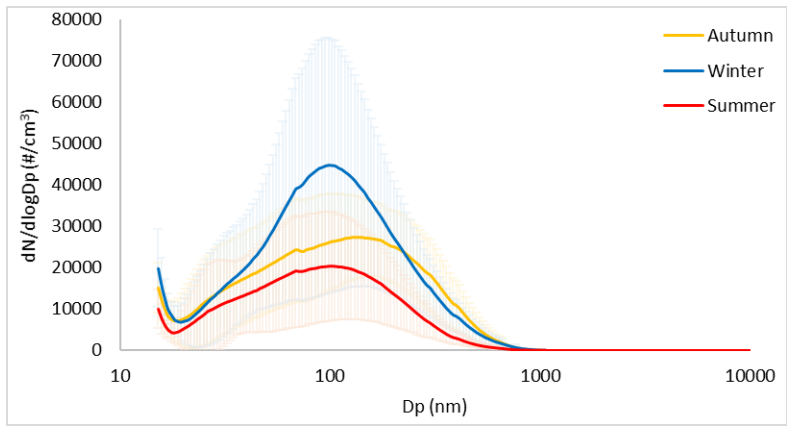
1053

1054 **Figure 6.** Seasonal average (line) and standard deviation (shadow) of particle number size
1055 distributions.
1056

1057
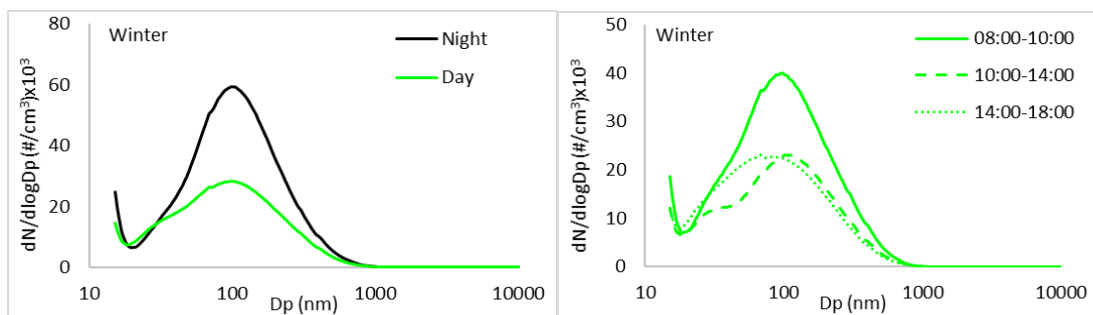
1058
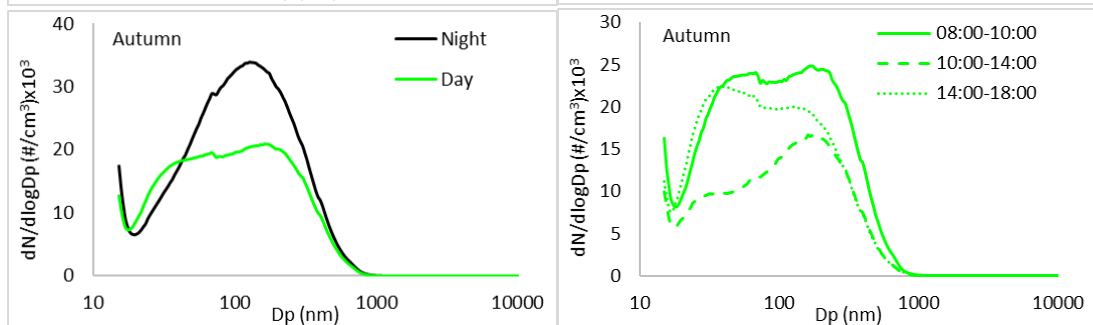
1059
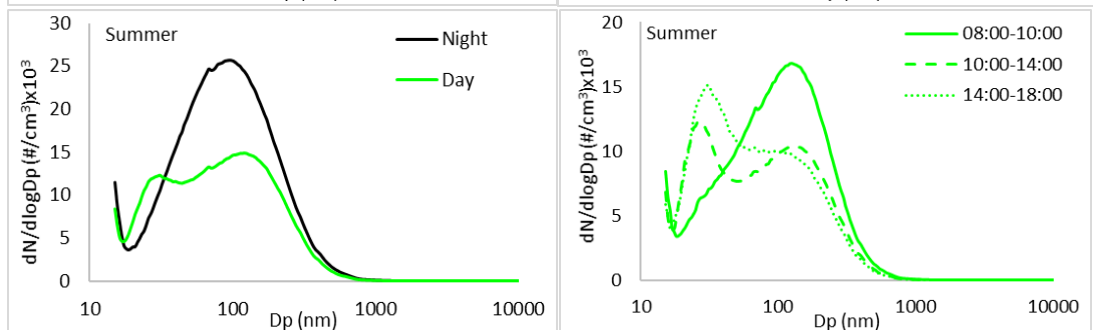
Figure 7. Hourly average day and night (left side) and during day hours (right side) particle number distributions in autumn, summer and winter in Delhi.

1060
1061
1062
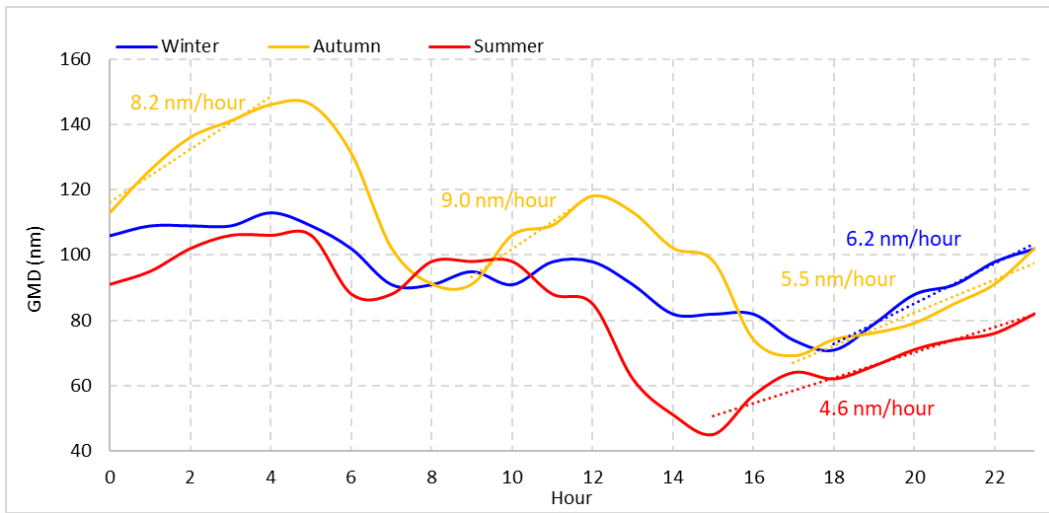
1063

1064 **Figure 8.** Diurnal change of the geometric mean diameter (GMD) calculated for winter, autumn
1065 and summer seasons. Growth rates (nm/hour) are calculated from dGMD/dt.
1066
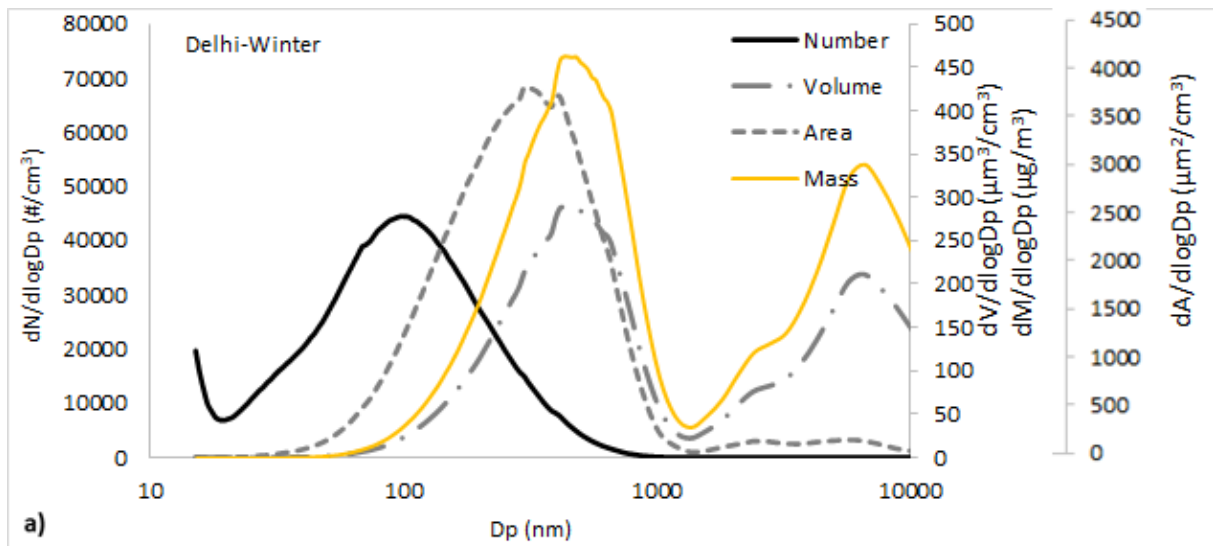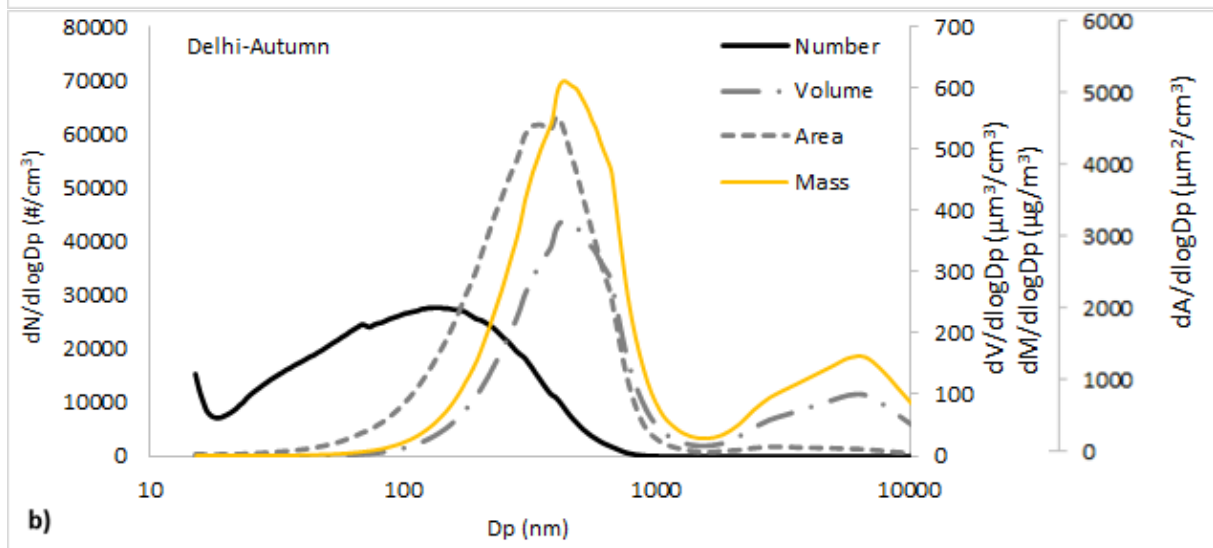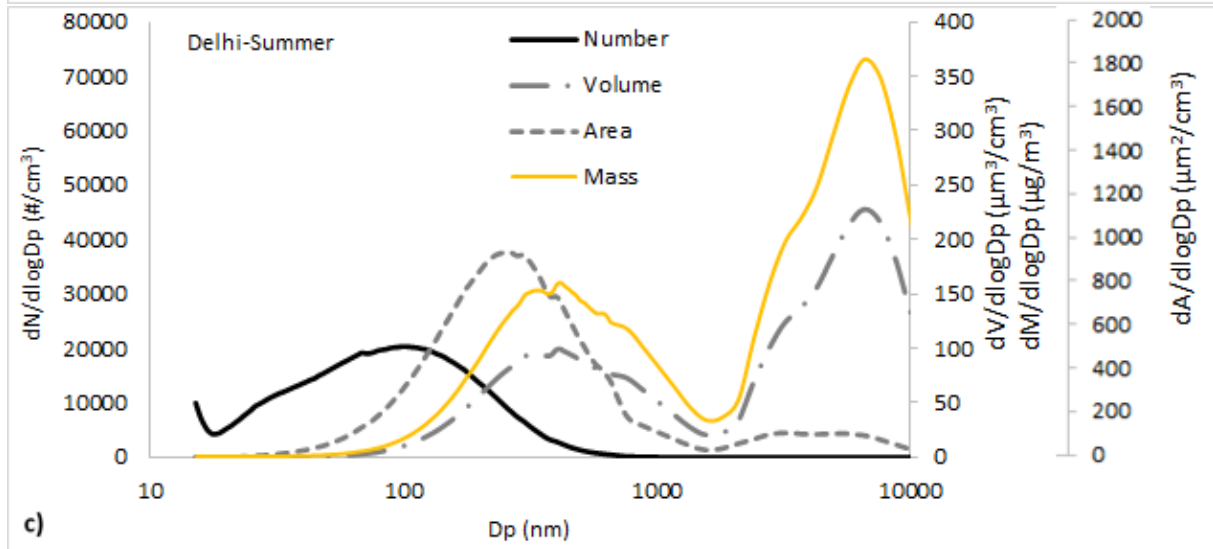
Figure 9. Hourly average particle number, volume and area distributions in the winter (a), autumn (b) and summer (c) in Delhi.
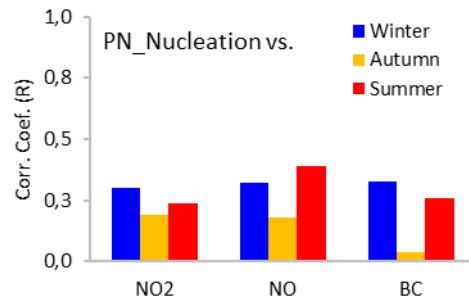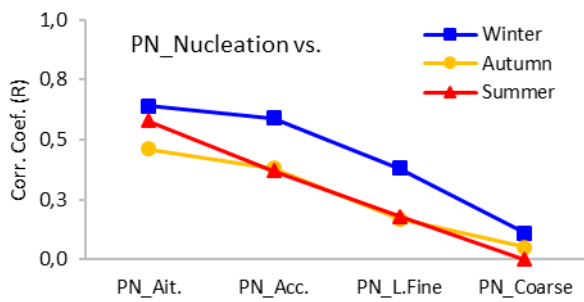
1073
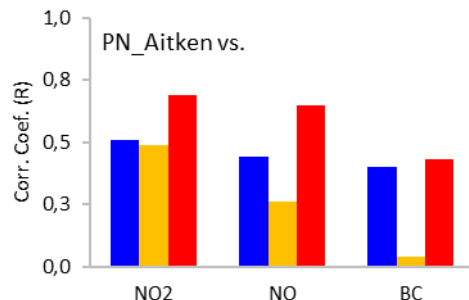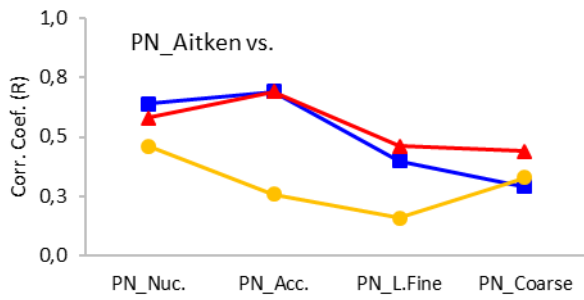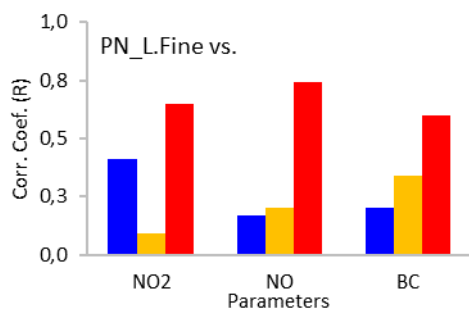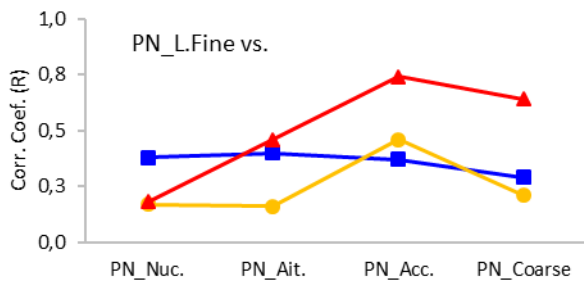
1074

1075

1076
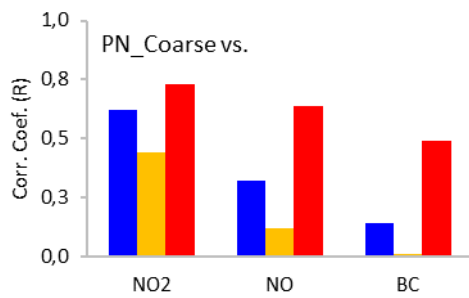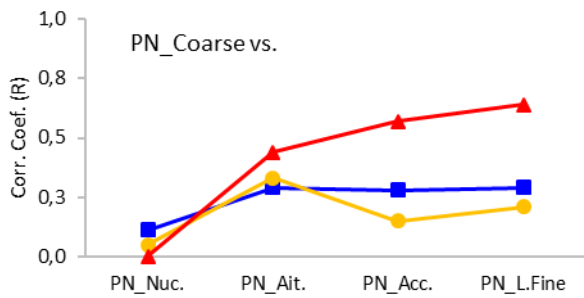
1077

1078

Figure 10. Correlation coefficient (R) between the hourly average PNs of five particle size fractions (left side) and NO, NO$_2$, BC (right side).

1079
1080
1081
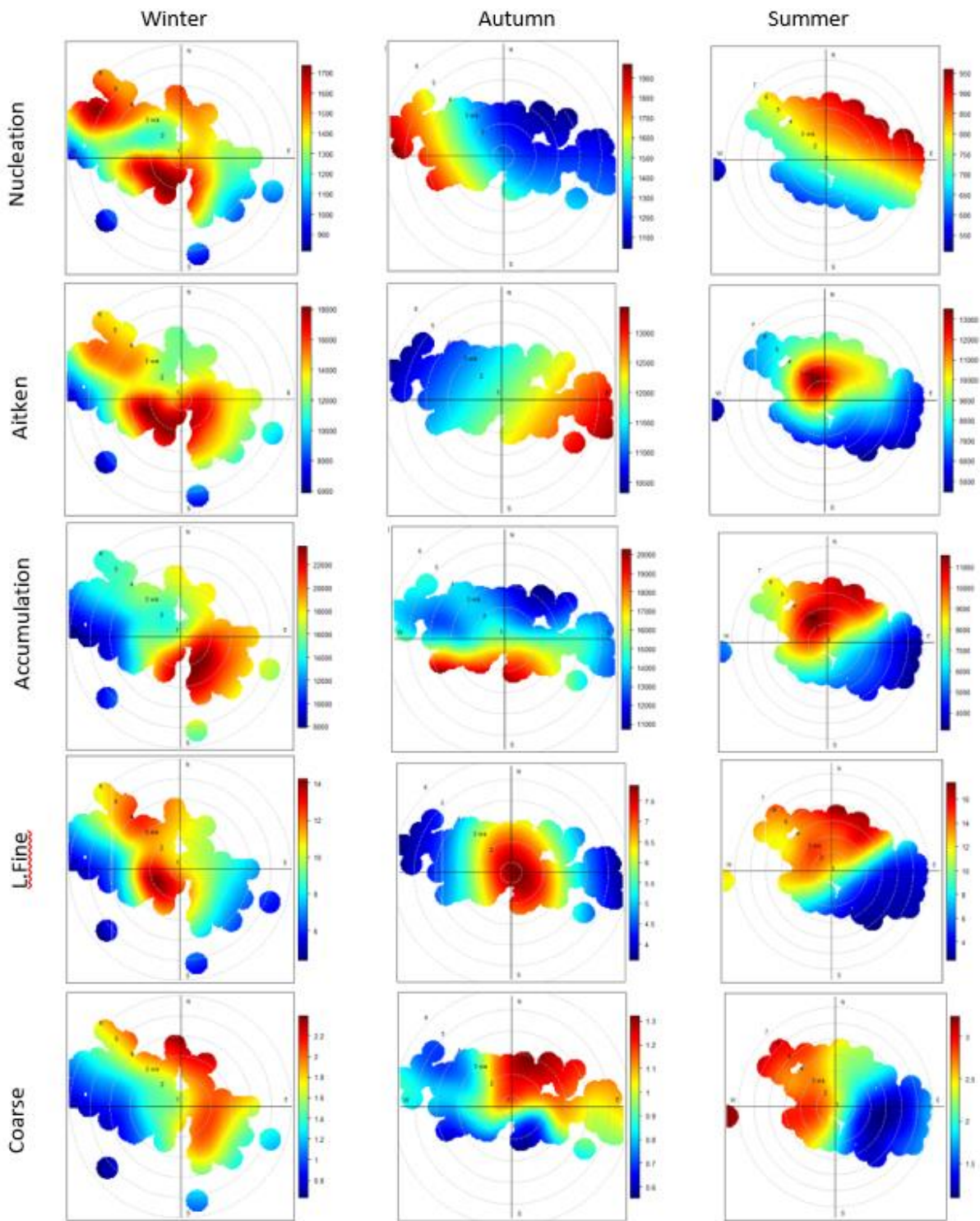
1082

1083

1084 **Figure 11.** Polar plots of PNs (#/cm^3) for five particle size fractions in winter, autumn and summer
1085 in Delhi.
1086